Somatic aging pathways regulate reproductive plasticity in *Caenorhabditis elegans*

Maria C. Ow, Alexandra M. Nichitean, and Sarah E. Hall[1]

Department of Biology, Syracuse University, Syracuse, NY 13244 USA

[1]Corresponding author: shall@syr.edu

Summary

Early life stress of an animal often results in changes in gene expression that correspond with changes in their adult phenotype. In the nematode *C. elegans*, starvation during early larval stages promotes entry into a non-feeding, stress-resistant stage named dauer until environmental conditions improve. Here we show that the endocrine signaling attributed to the somatic aging pathways in *C. elegans* adults lacking a functional germline also regulate the reproductive phenotypes of adults that have experienced dauer as a result of early life starvation. Postdauer adults modulate their fatty acid metabolism in order to re-allocate fat reserves in a manner benefitting their progeny at the expense of the parental somatic fat reservoir. Our results also show that the metabolic plasticity in postdauer animals and the inheritance of ancestral starvation memory in the progeny are a result of crosstalk between somatic and reproductive tissues mediated by the HRDE-1 nuclear RNAi Argonaute.

Keywords: *C. elegans*, postdauer, *daf-16*, *daf-12*, *nhr-49*, *hrde-1*, starvation, dauer, endocrine signaling, somatic aging

40 **Introduction**

41 Evidence indicating that experiences during early development affect behavior
42 and physiology in a stress-specific manner later in life is abundant throughout the
43 animal kingdom (Telang and Wells, 2004; Weaver et al. 2004; Binder et al. 2008;
44 Pellegroms et al. 2009; van Abeelen et al. 2012; Zhao et al. 2014; Canario et al. 2017;
45 Dantzer et al. 2019; Vitikainen et al. 2019). Epidemiological studies and studies using
46 mammalian animal models have supported the "thrifty" phenotype hypothesis which
47 proposes that fetal or postnatal malnutrition results in the increased risk for metabolic
48 disorders in the offspring (Neel, 1962; Hales and Barker, 1992; Vaag et al. 2012; Smith
49 and Ryckman, 2015). For instance, individuals exposed to the WWII Dutch Hunger
50 Winter during gestation had lower glucose tolerance and increased risk of obesity,
51 diabetes, and cardiovascular diseases in adulthood compared to siblings born before
52 the famine. In addition, the increased propensity to develop metabolic disorders was
53 inherited for two generations (Painter et al. 2008; Lumey et al. 2011; Veenendaal et al.
54 2013). Thus, understanding the relationship between fetal malnutrition and the
55 increased susceptibility to metabolic disorders in adulthood is critical for development of
56 intervention and therapeutic strategies.

57 The nematode *C. elegans* makes a critical decision regarding its developmental
58 trajectory based on the environmental conditions experienced during its first larval stage
59 (L1). If conditions are poor (e.g. low food availability, crowding, or high temperatures),
60 decreased insulin and TGF-β signaling in L1 larvae promote entry into an alternative,
61 stress-resistant, non-aging, diapause stage named dauer. Once conditions improve,
62 dauer larvae resume development as postdauer L4 larvae and continue through

63 reproductive adulthood as postdauer adults (Cassada and Russell, 1975). Alternatively,
64 if conditions are favorable, L1 larvae proceed through additional larval stages (L2-L4)
65 until reaching reproductive adulthood (control adults) (Sulston and Horvitz, 1977).
66 Although postdauer adults are morphologically similar to control adults, we previously
67 showed that postdauer adults retained a cellular memory of their early life experience
68 that resulted in genome-wide changes in their chromatin, transcriptome, and life history
69 traits (Hall et al. 2010, 2013; Ow et al. 2018). Remarkably, postdauer adults also
70 encoded the nature of their L1 environmental experience and gauged their adult
71 reproductive phenotypes and genome-wide gene expression based on this memory
72 (Ow et al. 2018). Postdauer adults that experienced crowding or high pheromone
73 conditions exhibited increased fertility and upregulated expression of genes involved in
74 reproduction relative to control adults that never experienced crowding. In contrast,
75 postdauer adults that experienced starvation (PD_{Stv}) exhibited decreased fertility and an
76 enrichment in somatic gene expression compared to control adults that never
77 experienced starvation (CON_{Stv}) (Ow et al. 2018). Moreover, the changes in fertility and
78 somatic gene expression in PD_{stv} adults required a functional germ line (Ow et al. 2018).
79 The prerequisite of crosstalk between somatic and reproductive tissues for the
80 postdauer reproductive phenotypes is also a key regulatory feature governing adult
81 lifespan and stress response (Kenyon 2010, 2010b). In *C. elegans*, endocrine signaling
82 has emerged as one of the principal pathways extending the lifespan of animals lacking
83 a germ line due to either ablation of germ line precursor cells or a mutation in the *glp-*
84 *1*/Notch receptor gene. The two main effectors of endocrine signaling, the FOXO
85 transcription factor DAF-16 and the nuclear hormone receptor (NHR) DAF-12, are

86 required for the increased lifespan of germline-less animals and are regulated by the
87 physiological state of the animal (Hsin and Kenyon, 1999; Kenyon 2010, 2010b; Murphy
88 and Hu, 2013). When an animal experiences reproductive stress, including sterility,
89 DAF-16 is dephosphorylated and translocated to the nucleus where it can alter target
90 gene expression to promote the extended longevity of germ line-less animals (Kenyon
91 2010, 2010b; Murphy and Hu, 2013). DAF-12, a homolog of the mammalian vitamin D
92 receptor, binds to bile acid-like steroid ligands (dafachronic acids or DA) to promote the
93 expression of genes involved in reproduction and growth in favorable conditions (Antebi
94 2014). In *glp-1* mutants, the Δ^7 form of DA (Δ^7-DA) is four-fold increased compared to
95 wild-type and promotes DAF-16 nuclear localization (Berman and Kenyon, 2006; Shen
96 et al. 2012). One of the consequences of the DAF-16 and DAF-12 dependent endocrine
97 signaling in *glp-1* mutants is a significant increase in stored intestinal fat, which allows
98 for somatic maintenance and prolonged longevity in the absence of germline
99 development (Wang et al. 2008).

100 In this study, we show that steroid hormone signaling, reproductive longevity
101 signaling, and nuclear hormone receptors contribute to the decreased fertility of
102 postdauer animals that experienced early life starvation by regulating fatty acid
103 metabolism. The reproductive plasticity of PD_{stv} adults is a result of crosstalk between
104 somatic and reproductive tissues, the effect of which is an increase in lipid metabolic
105 pathway function in an animal that has experienced dauer, resulting in decreased
106 fertility but endowing metabolic robustness to their progeny. Thus, the pathways that
107 bestow increased lipid storage and extended longevity in a germline-less animal
108 function to promote reproduction in a postdauer animal that experienced early-life

109 starvation. We also show that the signals between the soma and the germ line are
110 dependent on HRDE-1, a germline-specific nuclear RNAi argonaute. Given the principal
111 role of HRDE-1 in RNAi-mediated transgenerational inheritance, this pathway may
112 transmit the ancestral starvation memory to an ensuing generation and provide the
113 necessary hardiness to survive future famine.
114
115

116 **Results**

117 *Dafachronic acid-dependent DAF-12 signaling is required for decreased fecundity after*
118 *starvation-induced dauer formation*

119 Given that endocrine signaling across tissues is a prominent feature of reproductive
120 longevity, we examined whether wild-type PD_{Stv} adults shared any gene expression
121 signatures with animals lacking a functional germ line. In *glp-1* mutants, increased
122 longevity is dependent on TOR (target of rapamycin) signaling, DAF-16/FOXO gene
123 regulation, steroid hormone signaling, and fatty acid metabolism regulation (Lapierre
124 and Hansen, 2012). With the exception of TOR signaling, we found significant gene
125 expression changes in PD_{Stv} adults of key genes in each of these regulatory pathways.

126 In the steroid signaling pathway, dafachronic acid (DA) biosynthesis requires the
127 cytochrome P450 DAF-9, the Reiske-like oxygenase DAF-36, and the hydroxysteroid
128 dehydrogenase HSD-1 (Fig. 1A) (Gerisch et al. 2004; Rottiers et al. 2006; Patel et al.
129 2008; Mahanti et al. 2014). In animals lacking a functional germ line, the levels of *daf-36*
130 mRNA and the Δ^7 form of DA (Δ^7-DA) are significantly increased compared to wild-type
131 (Shen et al. 2012). Interestingly, we found that in wild-type PD_{Stv} adults with a germ line,
132 *daf-36* mRNA is also increased 3-fold (p = 3.25e-04; FDR = 0.01) compared to control

133 adults (Ow et al. 2018). To investigate whether DA signaling plays a role in mediating
134 reproductive plasticity as a result of early life experience, we asked whether mutations
135 in DA biosynthesis genes would affect the reduced brood size observed in PD_{Stv} adults.
136 We found that *daf-9(rh50)* and *daf-36(k114)* strains, but not *hsd-1(mg433),* exhibited a
137 significant increase in brood size in PD_{Stv} adults, opposite of what we observed in wild-
138 type animals (Fig. 1B; Supplemental Table S1).

139 We next asked whether the steroid signaling that contributed to the reduced
140 fertility of PD_{Stv} adults acted through related NHRs, DAF-12 and NHR-8. Since null
141 mutants of *daf-12* are dauer defective, we used two *daf-12* alleles, *rh284* (Class 5
142 mutant) and *rh285* (Class 4 mutant), with lesions in the ligand binding domain (LBD)
143 that affect steroid signaling activity but otherwise have nearly normal dauer phenotype
144 (Antebi et al. 2000). Surprisingly, *daf-12(rh284)* and *daf-12(rh285)* exhibited a significant
145 increase in brood size, similar to that observed for the DA biosynthesis mutants (Fig.
146 1B; Supplemental Table S1). These results suggest that DA-dependent activity of DAF-
147 12 is required for reduced fertility in PD_{Stv} adults. The related gene *nhr-8* is also up-
148 regulated 2.5-fold in PD_{Stv} adults (Lindblom et al. 2001; Magner et al. 2013; Ow et al.
149 2018); however, *nhr-8(ok186)* exhibited a significant brood size reduction between
150 control and PD_{Stv} animals at levels comparable to wild-type N2 (Fig. 1B; Supplemental
151 Table S1). These results indicate that the reduced fertility of PD_{Stv} adults is dependent
152 on DA biosynthesis through DAF-9 and DAF-36 and the subsequent DA-binding activity
153 of DAF-12.

154 We next asked whether the exogenous addition of DA was sufficient to reduce
155 the brood size of PD_{Stv} adults. To test this hypothesis, we induced larva into dauer by

156 starvation with or without exogenously added 40 nM of Δ^7-DA and measured their brood
157 size. The addition of Δ^7-DA did not affect the fertility of wild-type and *daf-36(k114)* (Fig.
158 1C; Supplemental Table S2). However, *daf-9(rh50)* PD_{Stv} adults exhibited a significant
159 decrease in brood size in the presence of exogenous Δ^7-DA (Fig. 1C; Supplemental
160 Table S2). DAF-9 is reported to promote a feedback loop of DA production between the
161 neuroendocrine XXX cells and the hypodermis; thus, *daf-9* mutants may be more
162 sensitive to small changes in DA concentration (Antebi 2014). Taken together, these
163 results suggest that increased DA-dependent DAF-12 signaling is necessary, but
164 perhaps not sufficient, for the reduced brood size phenotype of PD_{Stv} adults.
165
166 *The DAF-16 reproductive longevity pathway mediates reproductive plasticity*
167 DAF-16 acts as a major effector of reduced insulin/IGF-1-like signaling (IIS) by
168 promoting the expression of a group of stress response genes (Class I targets) (Tepper
169 et al. 2013). PQM-1, a C2H2 zinc finger transcription factor, acts in a mutually
170 antagonistic manner to DAF-16 by up-regulating genes associated with growth and
171 reproduction (Class II targets), as its cellular localization in the nucleus is anti-correlated
172 to that of DAF-16 (Fig. 2A) (Tepper et al. 2013). Interestingly, we found that the set of
173 genes with significant changes in mRNA levels between PD_{stv} and controls was
174 enriched for DAF-16 Class I and Class II targets (Supplemental Results, Fig. S2A). In
175 addition, we found two genes that regulate DAF-16 cellular localization, *pqm-1* and *daf-*
176 *18*, were significantly up- and down-regulated, respectively, in PD_{stv} adults compared to
177 controls (Ow et al. 2018). DAF-18 the functional ortholog of the human PTEN tumor
178 suppressor gene that promotes the nuclear localization of DAF-16 (Ogg and Ruvkun,

179 1998; Gil et al. 1999; Mihaylova et al. 1999; Solari et al. 2005). Together, the overlap in
180 DAF-16 gene targets and the significant changes in the expression of *pqm-1* and *daf-18*
181 prompted us to ask whether PQM-1 and DAF-18 contribute to the reduced fertility in
182 PD_{Stv} adults by altering the regulation of genes involved in reproduction and
183 sequestering DAF-16 in the cytoplasm. We investigated this hypothesis by performing
184 brood assays on adults carrying mutations in *pqm-1* and *daf-18*. Surprisingly, the brood
185 sizes of control and PD_{Stv} adults in *pqm-1(ok485)* and *daf-18(e1375)* strains were
186 similar to wild type, indicating that gene regulation by PQM-1 is unlikely to contribute to
187 the PD_{Stv} decreased brood size phenotype (Fig. 2B; Supplemental Table S4). Since *daf-*
188 *18(e1375)* is a hypomorph, we next tested the possibility that DAF-16 localization may
189 play a role in regulating postdauer reproduction. *daf-16* null mutants are dauer
190 defective; thus, we asked whether a *daf-16(mu86)* null mutant expressing a rescuing
191 transgene (*daf-16a^{AM}::gfp*) that constitutively localizes DAF-16 to the nucleus would
192 show a brood size plasticity phenotype (Lin et al. 2001). Similar to what was observed
193 for *daf-18(e1375)*, the *daf-16(mu86); daf-16a^{AM}::gfp* transgenic strain displayed a
194 reduced brood size in PD_{Stv} similar to wild-type N2 (Fig. 2B; Supplemental Table S4).
195 These results suggest that the nuclear localization of DAF-16, and not PQM-1, may be
196 contributing to the diminished fertility phenotype of PD_{Stv} adults.

197 To further investigate whether the nuclear localization of DAF-16 is required for
198 the reproductive plasticity between control and PD_{Stv} animals, we measured the brood
199 size of animals with mutations in genes that regulate the cellular localization of DAF-16.
200 First, we tested SMK-1/PPP4R3A, which promotes the nuclear localization of DAF-16
201 when animals are exposed to pathogenic bacteria, ultraviolet irradiation, and oxidative

202 stress, but does not affect the dauer development and reproductive timing activities of
203 DAF-16 (Wolff et al. 2006). We found that *smk-1(mn156)* mutants continued to exhibit a
204 decreased PD_{Stv} fertility compared to controls. Secondly, we examined two genes, *kri-1*
205 (an ortholog of the human intestinal ankyrin-repeat protein KRIT1/CCM1) and *tcer-1* (a
206 homolog of the human transcription elongation factor TCERG1), that are required for
207 DAF-16 nuclear localization and extend adult lifespan in germ line-less animals, but do
208 not regulate dauer formation (Berman and Kenyon, 2006; Ghazi et al. 2009). We found
209 that decreased brood size in PD_{Stv} was abrogated in the *kri-1(ok1251)* and *tcer-*
210 *1(tm1452)* mutants (Fig. 2B; Supplemental Table S4). Because TCER-1 regulates the
211 transcription of its target genes in a DAF-16-dependent and independent manner (Armit
212 et al. 2016), these results indicate that KRI-1, TCER-1, and possibly DAF-16 are
213 required for the reproductive plasticity in PD_{Stv} animals.
214
215 *Increased fatty acid metabolism promotes PD_{Stv} fertility*
216 In animals lacking a germ line, DAF-16 and TCER-1 are required to bolster the
217 expression of lipid biosynthesis, storage, and hydrolysis genes to promote adult
218 longevity (Armit et al. 2016). Similar to germ line-less *glp-1* mutants, PD_{Stv} adults
219 exhibited a significant altered expression of ~26% (33 of 127 genes) of all the fatty acid
220 metabolic genes, including ~46% (18 of 39 genes) also targeted by DAF-16 and TCER-
221 1 (Fig. S2B; Supplemental Table S5). These results suggest that DAF-16 and TCER-1
222 play a role in regulating reproductive plasticity between controls and PD_{Stv} by up-
223 regulating fatty acid metabolism.

224 To investigate this hypothesis, we asked if mutations in known regulators of lipid
225 metabolism would exhibit changes in brood size in PD_{Stv} adults when compared to
226 controls. One of the genes jointly up-regulated by DAF-16 and TCER-1 is *nhr-49*, a
227 nuclear hormone receptor homologous to the mammalian HNF4α lipid sensing nuclear
228 receptor involved in the regulation of fatty acid metabolism and the oxidative stress
229 response (Ratnappan et al. 2014; Amrit et al. 2016; Moreno-Arriola et al. 2016; Goh et
230 al. 2018; Hu et al. 2018). Additional nuclear hormone receptors, NHR-80, NHR-13, and
231 NHR-66, and the Mediator complex subunit, MDT-15, partner with NHR-49 and co-
232 regulate the expression of genes involved in various aspects of lipid metabolism such
233 as fatty acid β-oxidation, transport, remodeling, and desaturation (Van Gilst et al. 2005a,
234 2005b; Taubert et al. 2006; Nomura et al. 2010; Pathare et al. 2012; Ratnappan et al.
235 2014; Folick et al. 2015; Amrit et al. 2016). In addition, SBP-1 (homolog of mammalian
236 SREBP) and NHR-49 are co-regulated by MDT-15 as part of a transcriptional network
237 coordinating the expression of delta-9 (Δ9) fatty acid desaturase genes (Fig. 3B) (Yang
238 et al. 2006; Taubert et al. 2006).

239 The reduced fertility of PD_{Stv} characteristic of wild-type animals was also
240 observed in *nhr-80(tm1011)*, *nhr-13(gk796)*, *nhr-66(ok940)*, and *mdt-15(tm2182)*
241 strains, but not in *sbp-1(ep79)* (Fig. 3A; Supplemental Table S6). In addition, two *nhr-49*
242 *loss-of-function* (*lof*) mutants, *nhr-49(nr2014)* and *nhr-49(gk405)*, failed to exhibit the
243 decreased fertility in PD_{Stv} adults compared to CON_{Stv}, while a third *nhr-49(ok2165) lof*
244 allele continued to display a PD_{Stv} reduction in brood size (Fig. 3A; Supplemental Table
245 S6). Because the three *nhr-49* mutant alleles, *nr2014*, *gk405*, and *ok2165*, differ in the
246 nature and the location of their lesions (Lee et al. 2016), their biological function may

247 vary and hence result in phenotypic differences (*nr2041* and *gk405* vs. *ok2165*).
248 Animals expressing *nhr-49* gain-of-function alleles (*et7*, *et8*, and *et13*) with missense
249 lesions located at or near the LBD may augment NHR-49 activity resulting in a
250 reproductive plasticity phenotype comparable to that of wild-type N2 (Fig. 3A;
251 Supplemental Table S6) (Svensk et al. 2013; Lee et al. 2016). Because of the
252 interaction between NHR-49, NHR-80, NHR-13, and NHR-66, we also examined if
253 double and triple mutants of these NHRs would have any reproductive plasticity
254 phenotypes. Double and triple mutant combinations of alleles exhibited an abolishment
255 of the PD_{Stv} decreased brood size phenotype only if they expressed the *nhr-49(nr2041)*
256 mutation (Fig. 3C; Supplemental Table S7). Thus far, our results indicate that NHR-49
257 and SBP-1 are important in the reproduction program of PD_{Stv} adults, likely by up-
258 regulating fat metabolism genes.
259 NHR-49 and SBP-1 up-regulate the expression of genes involved in fatty acid
260 biosynthesis, including the Δ9 desaturases, *fat-5*, *fat-6*, and *fat-7*, and the delta-12 (Δ12)
261 desaturase *fat-2* (Nomura et al. 2010; Han et al. 2017). FAT-5, FAT-6, and FAT-7
262 convert saturated fatty acids (SFAs) to mono-unsaturated fatty acids (MUFAs), while
263 FAT-2 catalyzes the conversion of MUFAs to poly-unsaturated fatty acids (PUFAs)
264 (Watts and Ristow, 2017). Our previous mRNA-Seq results showed that the expression
265 of *fat-5*, *fat-6*, *fat-7*, and *fat-2* increased significantly between 3.8- and 26.6-fold in wild-
266 type PD_{Stv} adults compared to controls (Ow et al. 2018). While strains expressing a
267 single *fat-5(tm331)*, *fat-6(tm420)*, *fat-7(wa36)*, or *fat-2(wa17)* mutation continued to
268 exhibit the reduced brood size phenotype in PD_{Stv} adults, double mutants expressing a
269 mutation in *fat-6* no longer displayed the reduced PD_{Stv} phenotype. The double mutant

270 *fat-7(wa36); fat-5(tm331)* continued to display a significant fertility difference between
271 controls and PD_{Stv} (Fig. 3D; Supplemental Table S8). These results suggest: 1) a
272 functional redundancy between the Δ9 fatty acid desaturases in modulating lipid
273 homeostasis of PD_{Stv} adults, with FAT-6 playing a more principal role than FAT-5 and
274 FAT-7; and 2) MUFAs are required for the decreased fertility phenotype in PD_{Stv} adults
275 compared to controls.

276 In *C. elegans*, MUFAs are essential for viability as a triple *fat-5; fat-6; fat-7*
277 mutant is lethal (Brock et al. 2006). MUFAs, such as oleic acid, can be remodeled to
278 become PUFAs, phospholipids, and neutral lipids such as triacylglycerols (TAGs), which
279 serve as energy storage molecules in the intestine, hypodermis, and germ line (Watts
280 and Ristow, 2017). In addition to acting as key regulators of fat metabolism, FAT-5,
281 FAT-6, and FAT-7 are also essential in promoting the long lifespan of adult worms
282 lacking a germ line (Van Gilst et al. 2005a; Brock et al. 2006; Goudeau et al. 2011;
283 Ratnappan et al. 2014). Given that MUFAs are required for the reduced fertility of PD_{Stv}
284 adults compared to controls, we asked whether the dietary addition of oleic acid to PD_{Stv}
285 animals would further reduce their brood size such that they would produce even fewer
286 progeny compared to PD_{Stv} animals not supplemented with oleic acid. To test this
287 hypothesis, we compared the brood size of PD_{Stv} adults fed *E. coli* OP50 grown with
288 oleic acid and PD_{Stv} adults whose bacterial diet was not pre-loaded with oleic acid. We
289 tested the N2 wild-type, *nhr-49(nr2041)*, *nhr-49(gk405)*, and *nhr-49(nr2041); nhr-*
290 *80(tm1011)* strains, and found that for all genotypes, the supplementation of oleic acid
291 significantly increased the progeny number produced by PD_{Stv} compared to PD_{Stv} adults
292 on the control diet (Fig. 3E; Supplemental Table S9). These results indicate that oleic

293 acid is a limiting factor for reproduction, even for wild-type animals, after passage
294 through the starvation-induced dauer stage. Altogether, these results suggest that NHR-
295 49 and SBP-1 are critical for the decreased fertility in PD_{Stv} adults by mediating the up-
296 regulation of fatty acid desaturases and promoting the synthesis of sufficient levels of
297 oleic acid needed for reproduction after the animals experienced starvation-induced
298 dauer formation.
299
300 *Starvation-induced postdauer adults have reduced fat stores*
301 In long-lived *glp-1* mutants lacking a germ line, fat stores are increased relative to wild-
302 type (Steinbaugh et al. 2015; Amrit et al. 2016). Given that PD_{Stv} adults also have an
303 increased expression of lipid metabolism genes similar to *glp-1* adults, but have limited
304 quantities of oleic acid for reproduction, we questioned what the status of fat stores
305 would be in wild-type adults with an intact germ line that had passed through dauer due
306 to starvation. Using Oil Red O (ORO) staining, we compared the amounts of neutral
307 triglycerides and lipids (O'Rourke et al. 2009) in PD_{Stv} one-day-old adults and age-
308 matched control adults. Interestingly, PD_{Stv} adults have a significantly reduced amount
309 of stored lipids relative to control adults in their intestine, but still displayed ORO
310 staining in the embryos within the uterus (Fig. 4A, 4B). These results are consistent with
311 a model that PD_{Stv} adults have increased expression of lipid metabolism genes in order
312 to produce sufficient levels of MUFAs needed for reproduction rather than lipid storage.
313 Next, we investigated whether the decreased lipid stores in PD_{Stv} adults was
314 dependent upon DAF-12 and TCER-1. Both *daf-12(rh284)* and *daf-12(rh285)* mutants
315 displayed a significant increase in lipid storage in PD_{Stv} adults relative to control adults,

316 opposite to what was observed in wild-type, indicating that DA-mediated DAF-12 activity
317 is required for regulation of fat stores in PD_{Stv} adults (Fig. 4A, 4B). Interestingly, the
318 ORO staining positively correlated with brood sizes in wild-type N2 and the *daf-12*
319 mutants: fat stores and fertility decreased in wild-type PD_{Stv} adults, while fat stores and
320 fertility increased in *daf-12* PD_{Stv} adults compared to *daf-12* CON_{Stv} adults (Fig. 1B, 4A,
321 4B; Supplemental Table S1). In *tcer-1(tm1452*) adults, lipid staining was diminished in
322 PD_{Stv} compared to controls, similar to what is seen in wild-type (Fig. 4A, 4B). However,
323 since both *tcer-1* control and PD_{Stv} adults have reduced fat stores compared to their
324 wild-type counterparts, and TCER-1 is known to positively regulate NHR-49 and fatty
325 acid metabolism, this result is likely due to the inability of these animals to store fat and
326 not because the decreased fat stores in wild-type PD_{Stv} adults is TCER-1 independent.
327 In addition to regulation of fat metabolism genes in the intestine, TCER-1 also functions
328 redundantly with PUF-8, a member of an evolutionarily conserved stem cell proliferation
329 modulatory family, to potentiate germ cell proliferation in animals undergoing continuous
330 development (Pushpa et al. 2013). Thus, our *tcer-1(tm1452)* results suggest that TCER-
331 1 activity may also be necessary in regulating germline mechanisms that curtail fertility
332 following exit from dauer diapause.

333 During *C. elegans* reproduction, intestinal fat stores are reallocated into low-
334 density lipoproteins (LDL)-like particles (yolk lipoproteins or vitellogenins) that are
335 incorporated into oocytes through receptor-mediated endocytosis in a process called
336 vitellogenesis, and serve as the only supply of nutrients to the developing embryos
337 (Kimble and Sharrock, 1983; Grant and Hirsch, 1999). Six vitellogenins homologous to
338 the human ApoB proteins are encoded in the *C. elegans* genome, *vit-1* through *vit-6*,

339 and concomitant multiple RNAi knockdown of the *vit* genes increases adult lifespan in a
340 process that requires NHR-49 and NHR-80 (Spieth et al. 1991; Seah et al. 2016). The
341 transition from dauer to reproductive adulthood is an energetically costly process that
342 likely drains the already reduced fat reservoirs in dauers that experienced early-life
343 starvation. Because vitellogenesis mobilizes intestinal fat resources for reproduction
344 and depletes somatic lipid stores (Kimble and Sharrock, 1983), we hypothesized that
345 PD_{Stv} adults have reduced fat reservoirs because they prioritize vitellogenesis as a
346 reproductive investment over intestinal storage. To test this hypothesis, we examined
347 the fat stores in control and PD_{Stv} adults following RNAi knockdown of *vit-1,* which also
348 results in the knockdown of *vit-2/3/4/5* due to the high sequence homology amongst the
349 *vit* genes (Seah et al. 2016) (Supplemental Fig. S4). In the RNAi treated animals, PD_{Stv}
350 adults continued to exhibit decreased fat stores compared to control adults, similar to
351 the empty vector negative controls. However, PD_{Stv} adults treated with *vit* RNAi have
352 significantly greater intestinal fat deposits than PD_{Stv} negative controls ($p < 0.0001$),
353 indicating that increased vitellogenesis in PD_{Stv} adults may be one contributing factor to
354 the lack of stored intestinal fat (Fig. 4C, 4D). These results are consistent with our
355 previous finding that oleic acid is a limiting resource for reproduction in PD_{Stv} animals,
356 and suggests a model where PD_{Stv} adults utilize fat accumulated after diapause for
357 reproduction and not storage.
358
359 *Steroid signaling, reproductive longevity, and fatty acid metabolic pathways act*
360 *synergistically at different developmental time points to regulate reproductive plasticity*

361 Thus far, our results indicate that both DA-dependent DAF-12 activity and TCER-1 are
362 required for the reduced fertility phenotype in PD_{Stv} adults. However, the *daf-12* and
363 *tcer-1* PD_{Stv} mutant phenotypes are distinct, suggesting that they act in different
364 pathways, tissues, or developmental time points to regulate PD_{Stv} fertility. Furthermore,
365 the brood sizes of *kri-1(ok1251)* or *tcer-1(tm1425)* PD_{Stv} adults supplemented with
366 exogenous Δ^7-DA were unaffected, indicating that the effect of DA on PD_{Stv} brood size
367 is independent of the reproductive longevity pathway (Supplemental Fig. S3;
368 Supplemental Table S12). To further investigate the developmental mechanism of
369 steroid signaling, reproductive longevity, and fatty acid metabolism pathways in the
370 regulation of reproductive plasticity, we examined if DAF-12, TCER-1, and NHR-49 play
371 a direct role in the timing of germline proliferation in postdauer larvae. We previously
372 demonstrated that wild-type PD_{Stv} animals delay the onset of germline proliferation
373 compared to control animals, resulting in a reduced brood size (Ow et al. 2018). *C.*
374 *elegans* begins germ cell proliferation after hatching and continues throughout larval
375 development. Germ cells at the most distal ends of the gonad undergo mitotic self-
376 renewal while germ cells located more proximal in the gonad enter and undergo meiosis
377 (Kimble and Crittenden, 2005). In *C. elegans* hermaphrodites, undifferentiated germ
378 cells initiate spermatogenesis during the L4 larval stage, followed by a transition to
379 oogenesis at the adult stage (L'Hernault, 2006). Therefore, reproduction in *C. elegans*
380 hermaphrodites is sperm-limited (Byerly et al. 1976; Ward and Carrel, 1979; Kimble and
381 Ward, 1988). In previous results, when control and PD_{Stv} somatic development was
382 synchronized using vulva morphology, we observed significantly fewer germ cell rows in

383 PD_{Stv} larvae compared to control larvae, correlating with fewer sperm available for self-
384 fertilization in adulthood (Ow et al. 2018).

385 To determine if DAF-12, TCER-1, and NHR-49 play a direct role in germline
386 proliferation as a mechanism to regulate reproductive plasticity, we counted the number
387 of germ cell rows in control and PD_{Stv} mutant larvae that were developmentally
388 synchronized by their somatic morphology. Because *daf-12(rh284)* and *daf-12(rh285)*
389 mutants have altered germline morphologies that prevent accurate synchronization, we
390 used the *daf-36(k114)* mutation to disrupt the steroid signaling pathway. First, we
391 recapitulated our previous results showing that wild-type PD_{Stv} larvae have significantly
392 fewer total germ cell rows compared to control larvae due to reduced cell rows in the
393 meiotic transition zone (Fig. 5; Supplemental Fig. S6). In contrast, *daf-36(k114)* control
394 and PD_{Stv} larvae did not exhibit a significant difference in total (mitotic and meiotic) cell
395 rows, indicating that DAF-36-dependent DA is required during early germline
396 development for the delay in PD_{Stv} germ cell proliferation (Fig. 5; Supplemental Fig. S6).
397 This result is consistent with the increased brood size of PD_{Stv} adults in *daf-12(rh284)*
398 and *daf-12(rh285)* mutants, which express DAF-12 proteins unable to bind to DA.

399 In contrast to the *daf-36* mutant, the *nhr-49(nr2041)* mutant exhibited a significant
400 decrease in the number of total germ cell rows in PD_{Stv} larvae relative to control larvae,
401 similar to wild-type animals (Fig. 5). However, the numbers of germ cell rows in the
402 mitotic and meiotic zones of *nhr-49* control and PD_{stv} animals were not significantly
403 different (Supplemental Fig. S6). Since NHR-49 is required for the reduced fertility in
404 PD_{Stv} adults, these results suggest that NHR-49 plays a small role in regulating germline
405 proliferation in larvae, and a larger role in regulating fatty acid metabolism in the

406 intestine to support vitellogenesis in adults. Like NHR-49, TCER-1 plays a role in the
407 intestine acting to upregulate fatty acid metabolism genes in animals lacking germ cells,
408 but also plays a role in the regulation of germ cell proliferation (Pushpa et al. 2013;
409 Amrit et al. 2016). We found that a mutation in *tcer-1* resulted in a similar number of
410 total germ cell rows in control and PD_{Stv} larvae, indicating that TCER-1 plays a role in
411 PD_{Stv} reproductive plasticity by regulating germ cell proliferation in addition to its
412 intestinal role (Fig. 5). Interestingly, *tcer-1* PD_{Stv} larvae also appear to have a defect in
413 the onset of meiosis, since PD_{Stv} larvae have significantly great number of mitotic germ
414 cell rows compared to controls (Supplemental Fig. S6). Together, these results indicate
415 that DAF-12 steroid signaling and TCER-1 act early in germline development to delay
416 the onset of germ cell proliferation in PD_{Stv} animals, while NHR-49 primarily functions
417 later in development to promote the reduced fertility of PD_{Stv} adults.
418
419 *Generational transmission of early life starvation memory*
420 Our results suggest that PD_{Stv} upregulate their fatty acid metabolism to increase fat
421 transport to embryos. In humans, nutritional stress *in utero* not only promotes metabolic
422 syndrome in adulthood of the affected individuals, but also promotes obesity in
423 subsequent generations (Painter et al. 2008; Veenendaal et al. 2013). Therefore, to
424 examine whether the starvation-induced physiology of PD_{Stv} adults is inherited, we used
425 ORO staining to quantitate the fat storage in adult F_1 progeny of control and PD_{Stv}
426 adults that did not experience starvation themselves. Indeed, the adult F_1 progeny of
427 PD_{Stv} adults had an increased level of stored fat compared to F_1 progeny of control
428 adults (Fig. 6), but the difference was abolished by the F_2 generation. These results

429 indicate that the F_1 progeny of PD_{Stv} adults inherit a starvation memory that results in
430 metabolic reprogramming to increase their stored fat reserves.

431 In *C. elegans*, inheritance of gene expression states is often mediated by small
432 RNA pathways (Feng and Guang, 2013; Rechavi and Lev, 2017). The germline-specific,
433 nuclear Argonaute HRDE-1/WAGO-9 has been shown to promote transgenerational
434 silencing via the formation of heterochromatin at targeted genomic loci (Buckley et al.
435 2012; Feng and Guang, 2013; Rechavi and Lev, 2017). In particular, starvation-induced
436 L1 diapause has been shown to alter the small RNA populations of subsequent
437 generations in a HRDE-1 dependent manner (Rechavi et al. 2014). We examined
438 whether HRDE-1 was required for the generational inheritance of starvation memory by
439 quantifying fat storage in *hrde-1(tm1200)* mutant control and PD_{Stv} adults and their F_1
440 and F_2 progeny. First, we observed that the stored fat levels between *hrde-1* control and
441 PD_{Stv} adults were similar, suggesting that the germline-specific Argonaute is required for
442 decreased intestinal fat storage of PD_{Stv} adults (Fig. 6). In addition, the ORO staining of
443 the F_1 progeny of control and PD_{Stv} adults was also similar, indicating that HRDE-1 is
444 required for the generational inheritance of starvation memory (Fig. 6). Remarkably, in
445 the F_2 generation, the grand-progeny of *hrde*-1 PD_{Stv} mutants displayed increased ORO
446 staining like that observed for the F_1 generation of wild-type adults, suggestive of a
447 generational delay in the physiological response to ancestral early-life starvation upon
448 the loss of HRDE-1 activity (Fig. 6). Our genetic evidence suggests that the germline
449 nuclear RNAi pathway plays two roles: it contributes to the metabolic programming of
450 individuals that experienced early life starvation as well as promotes the generational
451 inheritance of starvation memory in the progeny. Our results show that *C. elegans*, like

452 humans, inherit the disposition for increased adiposity from parents that experienced
453 early life starvation.
454
455
456 **Discussion**
457 The trade-off between reproduction and longevity has long been associated with
458 the notion that in the absence of reproduction, the fat stores of an animal would be
459 redistributed to promote somatic maintenance (Williams 1966; Kirkwood 1977;
460 Westendorp and Kirkwood, 1998; Partridge et al. 2005). As such, reducing or
461 suppressing reproduction in animals often extends lifespan, in part due to enhanced
462 lipogenic processes (Fowler and Partridge 1989; Kenyon 2010, 2010b; Judd et al.
463 2011). What remains unclear is how reproduction and somatic maintenance are
464 balanced by developmental signals. In this study, we show that starvation early in the
465 life of a *C. elegans* animal with an intact reproductive system programs its transcriptome
466 to promote reproduction. Because dauers are non-feeding, starvation-induced dauers
467 have limited stored fat to survive the diapause stage and remodel out of dauer. We
468 propose a model whereby steroid signaling, reproductive longevity, and fatty acid
469 metabolic pathways are reprogrammed in animals that experienced starvation-induced
470 dauer in order to delay the onset of germline proliferation and redistribute intestinal fat
471 to developing oocytes (Fig. 7). These changes allow PD_{Stv} adults to delay reproduction
472 until energy thresholds are met to provide adequate levels of nutrition to fewer albeit
473 viable embryos at the expense of somatic survival and maintenance. In the absence of
474 a functional germ line, the fat that would normally be allocated to the progeny is

475 channeled to nurture somatic tissues and, consequently, extend adult lifespan. Thus,
476 the mechanisms that prolong lifespan in the absence of a functional germ line are the
477 same cellular programs deployed to respond to developmental signals triggered by
478 starvation early in life history in an animal capable of reproduction.

479 The extended lifespan associated with animals missing a functional germ line is
480 specifically dependent on the lack of proliferating germ cells and not due to sterility
481 resulting from sperm, oocyte, or meiotic precursor cell deficiency (Hsin and Kenyon,
482 1999; Arantes-Oliveira et al. 2002). Animals without a functional germ line have up-
483 regulated fat metabolism pathways and exhibit increased levels of intestinal fat stores
484 that are associated with a longer lifespan (Kenyon 2010, 2010b; Amrit et al. 2016).
485 Postdauer adults that experienced early life starvation have a delay in the onset of germ
486 cell proliferation after dauer exit and similarly have upregulated fat metabolism
487 pathways in adulthood. These results indicate that the cellular mechanisms that
488 promote germline proliferation during a critical period in development also negatively
489 regulate lipid metabolism, leading to altered somatic fat accumulation and longevity
490 (Wang et al. 2008). While a number of genes and cellular components affecting
491 germline proliferation have been extensively investigated (Kimble and Crittenden,
492 2005), what might the actual signals communicating the state of proliferating germ cells
493 be that arbitrate lipid levels and the aging process? Because upregulation of DAF-36
494 and Δ^7-DA is crucial for aging extension in germline-less animals and reproductive
495 plasticity in PD_{Stv} adults, it is likely that the signal communicating the state of germ cell
496 proliferation may include dafachronic acids. Dafachronic acids mediating increased
497 longevity are produced in the somatic gonad, which includes the stem cell niche site of

498 the germ line (Yamawaki et al. 2010). Based on our results, DA is required for the delay
499 in germline proliferation (Fig. 5), but DA-dependent DAF-12 activity is not necessary for
500 the increase in fatty acid metabolism observed in PD_{Stv} adults (Fig. 4A, 4B), suggesting
501 the possibility that dafachronic acids act in a DAF-12-independent manner to regulate
502 germ cell proliferation and fat metabolism. In addition, our results showed that *hrde-1* is
503 required for the altered fat metabolism in PD_{Stv} adults (Fig. 6), raising the possibility that
504 small RNAs could be another type of signaling molecule communicating the state of the
505 germ line to the soma. Small RNA pathways are potent surveillance mechanisms that
506 guard against the threat of foreign genetic invaders such as viruses and transposons
507 which can compromise germline integrity (Almeida et al. 2019). Because germ line
508 proliferation occurs throughout the lifetime of *C. elegans*, it is likely that small RNA
509 pathways survey the proliferative nature of the germ line at all stages of animal
510 development and potentially act as signaling molecules to regulate somatic processes
511 dependent upon the germ line.

512 One of the most intriguing findings of this study is that the starvation memory of
513 the parent is "bequeathed" to the F_1 progeny, triggering elevated levels of fat stores,
514 presumably as a physiological defense against ancestral famine (Fig. 6). Interestingly,
515 the increased intestinal fat inherited by the F_1 progeny of wild-type postdauer parents
516 bypassed the F_1 generation in the *hrde-1* mutant and was only evident in the F_2
517 generation (Fig. 6). One potential explanation is that small RNA signals are transmitted
518 to the F_1 generation via the HRDE-1 nuclear RNAi pathway to effect somatic
519 phenotypes. However, with the exception of DAF-16, none of the germline longevity
520 pathway genes or the vitellogenesis genes examined in this study are categorized as

521 direct HRDE-1 targets (Buckley et al. 2012). Given that the life stage (adulthood) at
522 which the HRDE-1 targets were identified is the same life stage that was used in this
523 study, we speculate that HRDE-1 may be indirectly targeting endocrine and
524 vitellogenins genes by: 1) targeting germ line genes that then affect somatic gene
525 expression; or 2) indirectly regulating the function of the endocrine and vitellogenin
526 genes by targeting a different repertoire of somatic targets. Interestingly, we find that
527 62% of small RNAs associated with HRDE-1 target genes (984 out of 1587) are
528 expressed in somatic tissues, such as neurons, intestine, hypodermis, and muscle
529 (Ortiz et al. 2014; Kaletsky et al. 2016). While silencing somatic genes in the germ line
530 is consistent with the described function of HRDE-1, our results raise the possibility that
531 HRDE-1 may also directly, or indirectly, target somatic genes. Accordingly, HRDE-1 is
532 known to contribute to the heritability of a cohort of small RNAs targeting nutrition and
533 lipid transporter genes that was inherited for at least three generations from populations
534 that experienced L1 larval arrest (Rechavi et al. 2014). In addition, HRDE-1 is required
535 for the repression of a group of genes activated upon multi-generational high
536 temperature stress that is inherited for at least two generations in the absence of the
537 stress (Ni et al. 2016). Thus, it is likely that HRDE-1 and the nuclear RNAi pathway may
538 serve as a signaling referee between the soma and the germ line to effect changes due
539 to environmental and developmental signals to perdure ancestral starvation memory.
540 Our study showed that PD_{Stv} adults have upregulated expression of lipid
541 metabolism genes as a means to load embryos with increased fat and potentially
542 protect progeny against future starvation conditions. Not only are fatty acids critical for
543 cell and organelle maintenance and efficient energy storage molecules but they can

544 regulate aging by acting as signaling molecules (e.g. as nuclear hormone receptor
545 ligands). Indeed, the lipid profiles in a number of species change as animals age
546 resulting in the acceleration of cell and tissue damage such that levels of certain lipids
547 can serve as aging biomarkers (Papsdorf and Brunet, 2019). Also, studies have
548 reported that fatty acids can alter animal physiology through the modification of
549 chromatin states either by the direct addition of lipid moieties to chromatin or by
550 activating signaling pathways that affect chromatin landscapes (Hansen et al. 2013;
551 Papsdorf and Brunet, 2019). Furthermore, MUFAs have been shown to be the link
552 between H3K4me3 modifiers and lifespan in *C. elegans*, while the inheritance of
553 epigenetic memory through soma-germline crosstalk in response to cellular stresses are
554 associated with the H3K4me3 modification complex (Tauffenberger and Parker, 2014;
555 Kishimoto et al. 2016; Han et al. 2017). Altogether, these studies provide an exciting
556 groundwork to examine how the chromatin states in PD_{Stv} animals correlate with
557 metabolic plasticity due to early life starvation across generations.

558 During the course of its natural history, *C. elegans* occupies ephemeral
559 environments such as rotting fruit or decomposing vegetation, where conditions and
560 food availability are highly unpredictable. The dauer larva affords *C. elegans* a survival
561 and dispersal strategy to escape harsh environmental conditions by often associating
562 with passing invertebrate carriers. Accordingly, *C. elegans* is often found in the wild as
563 dauers. Once a food source is found, dauers resume reproductive development to
564 colonize the new habitat. Upon exhaustion of resources and population expansion,
565 young larvae enter dauer and thereby repeating the boom and bust life cycle
566 (Schulenburg and Félix, 2017). Because of frequent environmental perturbations, an

adopted phenotypic plasticity strategy would ensure an advantage in species survival. The generation following a bust period would inherit the cellular programs for increased somatic lipid stores. It is thus remarkable that the cellular mechanisms to ensure survival of the species are fundamentally similar between humans and nematodes, two species that have diverged hundreds of millions of years ago, once again underscoring the relevance of a simple roundworm in understanding basic animal physiology.

Acknowledgments

We are grateful for the generous gift of dafachronic acid from Frank Schroeder and Pooja Gubibanda for advice on its use. We thank Leszek Kotula and Angelina Regua for access to their microscope, and Eleanor Maine for thoughtful comments on this manuscript. Strain BS1080 was kindly provided by Tim Schedl. This work was partially supported by a NIHR01GM129135 grant to S.E.H. We thank the CGC, which is funded by the NIH Office of Research Infrastructure Programs (P40 OD010440), for providing strains.

Author contributions

M.C.O. and S.E.H. conceived and designed experiments. M.C.O. and A.M.N. performed experiments. M.C.O., A.M.N., and S.E.H. analyzed the data. M.C.O. and S.E.H. wrote the manuscript.

590 **Declaration of interests**

591 The authors declare no competing interests.

592

593

594 **Figure legends**

595 **Figure 1.** Adult reproductive plasticity is dependent on DAF-12 steroid signaling. (*A*)
596 Model of DAF-12 NHR regulation of development. See text for details. (*B*) Brood size
597 comparison of PD_{Stv} relative to CON_{Stv} in wild-type N2 and mutant strains represented
598 as the mean ± S.E.M. ** $p < 0.01$, *** $p < 0.001$, **** $p < 0.0001$; Student's *t*-test;
599 comparison of PD_{Stv} to CON_{Stv} of a given genotype. $^{\&\&\&}$ $p < 0.001$, $^{\&\&\&\&}$ $p < 0.0001$; one-
600 way ANOVA with Fisher's LSD test; comparison of PD_{Stv}/CON_{Stv} brood size between
601 mutant and wild-type N2. Additional brood size data is provided in Supplemental Table
602 S1. (*C*) Brood size comparison of PD_{Stv} grown in the presence of 40 nM Δ^7-DA relative
603 to control, represented as the mean ± S.E.M. N= 4 trials, **** $p < 0.0001$ (Student's *t*-
604 test) indicates the comparison between PD_{Stv} with Δ^7-DA and control. $^{\&}$ $p < 0.05$ (one-
605 way ANOVA with Fisher's LSD *post hoc* test) refers to the comparison of brood size fold
606 change between *daf-9* and wild-type N2. Additional brood size data can be found in
607 Supplemental Table S2.

608

609 **Figure 2.** TCER-1 and KRI-1 regulate decreased fertility phenotype in PD_{stv} adults.
610 (*A*) Regulation of DAF-16 nuclear localization. See text for details. (*B*) Brood size
611 comparison of PD_{Stv} relative to CON_{Stv} in wild-type N2 and mutant strains represented
612 as the mean ± S.E.M. ** $p < 0.01$, *** $p < 0.001$, **** $p < 0.0001$; Student's *t*-test;

613 comparison of PD_{Stv} and CON_{Stv} of a given genotype. $^{\&}$ $p < 0.05$, $^{\&\&\&\&}$ $p < 0.0001$; one-
614 way ANOVA with Fisher's LSD *post hoc* test; comparison of the PD_{Stv}/CON_{Stv} brood
615 size change between a given mutant genotype to wild-type N2. Additional brood size
616 data is provided in Supplemental Table S4.
617
618 **Figure 3.** NHR-49, SBP-1, and FAT-6 modulate adult reproductive plasticity. (*A,C,*
619 *D*) Brood size comparison of PD_{Stv} relative to CON_{Stv} for wild-type N2 and mutant
620 strains represented as the mean ± S.E.M. Additional brood size data is provided in
621 Supplemental Tables S6, S7, and S8. (*B*) Model of lipid metabolism regulators. See text
622 for details. (*E*) Brood size of PD_{Stv} wild-type N2 and mutant animals fed with *E. coli*
623 OP50 pre-loaded with or without 600 μM of oleic acid (OA), represented as the mean ±
624 S.E.M. Additional brood size data is provided in Supplemental Table S9. * $p < 0.05$, ** p
625 < 0.01, *** $p < 0.001$, **** $p < 0.0001$; Student's *t*-test; comparison of PD_{stv} and CON_{stv}
626 brood size within a given genotype. $^{\&}$ $p < 0.05$, $^{\&\&\&\&}$ $p < 0.0001$ and n.s. (no
627 significance); one-way ANOVA with Fisher's LSD post hoc test; comparison of
628 PD_{Stv}/CON_{Stv} brood size between a given genotype to wild-type N2.
629
630 **Figure 4.** Fat stores are reduced in wild-type postdauer adults that experienced
631 starvation-induced dauer. (*A, C*) Oil Red O (ORO) intensity in CON_{Stv} and PD_{Stv} adults,
632 represented as violin plots with the mean (dashed line), first, and third quartiles
633 indicated (dotted lines). (*A*) **** $p < 0.0001$; Student's *t*-test; comparison between
634 CON_{Stv} and PD_{Stv} of the same genotype. $^{\&\&\&\&}$ $p < 0.0001$; one-way ANOVA with Fisher's
635 LSD *post hoc* test comparing mutant CON_{stv} or PD_{stv} to wild-type N2. n.s.; no

636 significance. Total sample size is indicated by *n*. (*C*) **** $p < 0.0001$; Student's *t*-test;
637 comparison between CON_{Stv} and PD_{Stv} of the same condition. && $p = 0.0038$ and &&&& p
638 < 0.0001; Student's *t*-test; comparison of CON_{stv} or PD_{stv} *vit-1* RNAi to empty RNAi
639 vector control. (*B, D*) Representative micrographs of one-day-old adults stained with
640 ORO.
641
642 **Figure 5.** DAF-12 and TCER-1 regulate the onset of germline proliferation. Total
643 germ cell rows in CON_{Stv} and PD_{Stv} wild-type N2 and mutant larva exhibiting L3 vulva
644 morphology (see Materials and methods). Data represented as violin plots with the
645 mean (dashed line), first, and third quartiles indicated (dotted lines) ** $p < 0.01$; **** $p <$
646 0.0001; Student's *t*-test. Total sample size is indicated by *n*.
647
648 **Figure 6.** Generational inheritance of starvation memory. *(A)* Intensity of ORO lipid
649 staining of wild-type N2 and *hrde-1(tm1200)* control and postdauer P_0, F_1, and F_2
650 generations, represented as violin plots with the mean (dashed line), first, and third
651 quartiles indicated (dotted lines). **** $p < 0.0001$; Student's *t*-test. n.s.; no significance.
652 Total sample size is indicated by *n*. (*B*) Representative micrographs of N2 and *hrde-*
653 *1(tm1200)* CON_{Stv} and PD_{Stv} P_0, F_1, and F_2 worms stained with ORO.
654
655 **Figure 7.** Model depicting endocrine signaling pathways acting as contributors to
656 fatty acid metabolism of PD_{stv} animals. Signaling between the soma and the germ line
657 establishing metabolic plasticity and the transmission of ancestral starvation memory
658 are dependent on HRDE-1.

STAR ★ METHODS

Detailed methods are provided in the online version of this paper and include the following:

- KEY RESOURCES TABLE
- CONTACT FOR REAGENT AND RESOURCE SHARING
- EXPERIMENTAL MODEL AND SUBJECT DETAILS
  - *C. elegans* strains and husbandry
- METHOD DETAILS
  - Plasmid construction and transgenic strains
  - Brood assays
  - Oil Red O staining
  - RNA interference
  - Dafachronic acid supplementation
  - Oleic acid supplementation
  - Germ cell rows
  - RNA extraction
  - Quantitative reverse transcription real-time PCR
- QUANTIFICATION AND STATISTICAL ANALYSIS
- DATA AND SOFTWARE AVAILABILITY

691 CONTACT FOR REAGENT AND RESOURCE SHARING

692 Further information and requests for resources and reagents should be directed to and
693 will be fulfilled by the Lead Contact, Sarah E. Hall (shall@syr.edu).

694 EXPERIMENTAL MODEL AND SUBJECT DETAILS

695 ***C. elegans* strains and husbandry**
696
697 N2 Bristol wild-type strain was used as the reference strain. Worms were grown at 20°C
698 unless otherwise indicated in Nematode Growth Medium (NGM) seeded with
699 *Escherichia coli* OP50 using standard methods (Brenner et al. 1974; Stiernagle 2006).
700 Mutants that were not previously backcrossed were backcrossed at least four times to
701 our laboratory N2 wild-type before use. All strains used in this study are listed in the Key
702 Resources Table.

703
704 METHOD DETAILS
705
706 **Plasmid construction and transgenic strains**
707
708 To clone P*glp-4::glp-4 cDNA::gfp::glp-4* 3'UTR, primers sets MO2454 & MO2455;
709 MO2516 & MO2507; MO2508 & MO2468; MO2469 & MO2470; and MO2471 &
710 MO2472 were used to amplify pUC19, 1.2 kb of the *glp-4* promoter, the *glp-4* cDNA
711 (using a cDNA library prepared from total RNA of a mixed N2 population as template),
712 the *gfp* gene (using Fire vector pPD95.75 as the template), and 500 bp of the *glp-4*
713 3'UTR, respectively, using Phusion DNA polymerase (NEB). Assembly of PCR products
714 was done using the NEBuilder HiFi DNA Assembly (E2621) to generate pMO555. P*glp-*
715 *4::glp-4 cDNA::gfp::glp-4* 3'UTR was cloned into the pCFJ151 MosSCI vector to
716 generate plasmid pMO557 using primer sets MO2499 & MO2500 and MO2514 &

717 MO2504 to amplify pCFJ151and P*glp-4::glp-4 cDNA::gfp::glp-4* 3'UTR (using pMO555
718 as template), respectively, using Phusion DNA polymerase (NEB) and assembled with
719 the NEBuilder HiFi DNA Assembly. To clone P*nhx-2::glp-4 cDNA::gfp::glp-4* 3'UTR,
720 overlap extension PCR was done with primers MO2544 (*Xma*I) and MO2533 (with
721 genomic DNA as template); MO2534 and MO2532 (*Sbf*I) (with pMO555 as template).
722 The resulting amplicon was digested with *Xma*I and *Sbf*I and cloned into pUC19 to
723 generate pMO562. P*nhx-2::glp-4 cDNA::gfp::glp-4* 3'UTR was cloned into pCFJ151
724 using the NEBuilder HiFi DNA Assembly and PCR products from primers MO2509 &
725 MO2504 (with pMO562 as template) and primers MO2499 & MO2500 (with pCFJ151 as
726 template) to create pMO565. To clone P*pgl-1::glp-4 cDNA::gfp::glp-4* 3'UTR, overlap
727 extension PCR was done with primers MO2545 (*Xma*I) and MO2536 (with genomic
728 DNA as template); MO2537 and MO2532 (*Sbf*I) (with pMO555 as template). The
729 resulting amplicon was digested with *Xma*I and *Sbf*I and cloned into pUC19 to generate
730 pMO559. P*pgl-1::glp-4 cDNA::gfp::glp-4* 3'UTR was cloned into pCFJ151 using the
731 NEBuilder HiFi DNA Assembly and PCR products from primers MO2510 & MO2504
732 (with pMO559 as template) and primers MO2499 & MO2500 (with pCFJ151 as
733 template) to create pMO566. To clone P*zfp-2::glp-4 cDNA::gfp::glp-4* 3'UTR, overlap
734 extension PCR was done with primers MO2546 (*Xma*I) and MO2538 (with genomic
735 DNA as template); MO2539 and MO2532 (*Sbf*I) (with pMO555 as template). The
736 resulting amplicon was digested with *Xma*I and *Sbf*I and cloned into pUC19 to generate
737 pMO560. P*zfp-2::glp-4 cDNA::gfp::glp-4* 3'UTR was cloned into pCFJ151 using the
738 NEBuilder HiFi DNA Assembly and PCR products from primers MO2511 & MO2504
739 (with pMO560 as template) and primers MO2499 & MO2500 (with pCFJ151 as

740 template) to create pMO567. Plasmids pMO557, pMO565, pMO566, and pMO567 were
741 used to generate single copy insertions, *pdrSi1* (*Pglp-4::glp-4 cDNA::gfp::glp-4 3'UTR*),
742 *pdrSi2* (*Pnhx-2::glp-4 cDNA::gfp::glp-4 3'UTR*), *pdrSi3* (*Pzfp-2 ::glp-4 cDNA::gfp::glp-4*
743 *3'UTR*), and *pdrSi4* (*Ppgl-1::glp-4 cDNA::gfp::glp-4 3'UTR*) by Mos1-mediated single
744 copy insertion (MosSCI) (Frokjaer-Jensen et al. 2008). All primers sequences are listed
745 in the Key Resources Table. Following integration into *unc-119(ed3)* animals
746 segregated from EG6699 [*ttTi5605 II; unc-119(ed3) III; oxEx1578* (*eft-3p::gfp* + *Cbr-unc-*
747 *119*)] that have lost the *oxEx1578* array, MosSCI insertions were genetically crossed
748 into the *glp-4(bn2)* background.
749
750 **Brood assays**
751
752 Ten L4 larvae were placed individually onto 35mm NGM plates seeded with *E. coli*
753 OP50 and incubated at 20°C. Animals were transferred daily to fresh 35mm NGM plates
754 until egg laying ceased. Live progeny from each egg laying plate were counted. Assays
755 were done from at least three biological independent replicates.
756
757 **Oil Red O staining**
758 Fat stores were stained using Oil Red O (ORO) dye as described by O'Rourke et al.
759 2009. Age matched one-day-old adults were washed from 60mm seeded NGM plates
760 with 1x PBS pH 7.4 and rinsed 3-4 times until they were cleared of bacteria. Worms
761 were permeabilized in 1x PBS pH 7.4 with an equal volume of 2x MRWB buffer (160
762 mM KCl, 40 mM NaCl, 14 mM Na_2EGTA, 1 mM spermidine-HCl, 0.4 mM spermine, 30
763 mM PIPES pH 7.4, 0.2% β-mercaptoethanol) and supplemented with 2%
764 paraformaldehyde. Samples were rocked for 1 hour at room temperature. Following

765 fixation, worm samples were washed with 1x PBS pH7.4, resuspended in 60%
766 isopropanol, and incubated at room temperature for 15 minutes. An Oil Red O (ORO)
767 stock solution (prepared beforehand as a 0.5 g/100 mL in isopropanol and equilibrated
768 in the dark at room temperature at least several days) was diluted to 60% with dH_2O
769 and rocked for at least one day to be used as the working stock. The ORO working
770 stock was filtered through a 0.22 um filter immediately before use. Fixed worms were
771 incubated in filtered ORO working stock and rocked overnight at room temperature.
772 Next day, worm samples were allowed to settle and the ORO stain was removed. Worm
773 pellets were washed once with 1x PBS pH7.4 and resuspended in 200 μL of 1x PBS
774 with 0.01% Triton X-100. Aliquots of worm samples were mounted onto microscope
775 glass slides and imaged.
776 Images were captured with either a Nikon Eclipse Ci with Spot 5.2 software or with an
777 iPhone through iDu Optics® equipped with a LabCam® adapter (New York, NY, USA).
778 Color images were separated into their RGB channel components and the intensity
779 measured on the green channel (Yen et al. 2010) using ImageJ (NIH).
780

781 **RNA interference**

782 Gravid adults were treated with hypochlorite to obtain embryos using standard methods
783 (Stiernagle 2006). Embryos were placed on NGM plates supplemented with 1mM IPTG
784 and 50 μg/ml carbenicillin seeded with a 10x concentrated bacterial culture expressing
785 the *k09f5.2* (*vit-1*) RNAi clone obtained from the Ahringer library (Kamath et al. 2001).
786 Embryos were allowed to grow until adulthood at which time they were treated again

787 with hypochlorite to obtain embryos. The recovered embryos were grown until day one
788 of adulthood and collected for ORO staining.
789
790 **Dafachronic acid supplementation**
791 The Δ^7 form of dafachronic acid (Δ^7-DA) (a kind gift from Frank Schroeder) was added
792 to a freshly grown culture of *E. coli* OP50 at a concentration of 40 nM and immediately
793 seeded onto NGM plates. NGM plates supplemented with an equivalent volume of
794 ethanol (the Δ^7-DA solvent) to those of the Δ^7-DA-supplemented NGM plates were used
795 as the control plates. Seeded plates were allowed to dry overnight before use.
796
797 **Oleic acid supplementation**
798 Animals were induced into dauer by starvation on peptone-less NGM plates seeded
799 with *E. coli* OP50 pre-loaded with oleic acid (NuChek Prep, Inc.; Elysian, Minnesota,
800 USA) as described by Devkota et al. 2017. OP50 was grown overnight at 37°C in liquid
801 LB supplemented with 600 μM of oleic acid or with an equivalent volume of ethanol (the
802 oleic acid solvent) to serve as the control. Cultures were pelleted and washed several
803 times with M9 buffer (Stiernagle, 2006) and resuspended at a 10x concentration. The
804 10x OP50 was seeded onto peptone-less NGM plates and allowed to dry overnight
805 before use.
806
807 **Germ cell rows**
808 All worm strains used for germ cell row counting have the integrated transgene *gld-*
809 *1*::*gfp*::*3xFLAG* from the BS1080 strain in their genetic background. Worms with L3

810 vulva morphology were identified by using Nomarski DIC microscopy at 630x (Seydoux
811 et al. 1993) and DAPI stained using the standard whole worm DAPI staining protocol.
812 The stained worms were imaged using a Leica DM5500B microscope with a
813 Hamamatsu camera controller C10600 ORCA-R2. When performing the germ cell row
814 counts, the start of the transition was identified when at least two cells in a row exhibited
815 the crescent-shaped nuclei morphology (Shakes et al. 2009).
816
817 **RNA extraction**
818 Total RNA was extracted using TRIzol Reagent (Life Technologies). Four volumes of
819 TRIzol reagent were added to a frozen worm pellet followed by vigorous vortexing for 20
820 minutes. Samples were centrifuged in a tabletop centrifuge at maximum speed and the
821 cleared supernatant was transferred to a fresh tube. The RNA was precipitated with
822 equal volume of isopropanol at -80°C for at least 30 minutes. RNA pellets were washed
823 with cold 75% ethanol, dried, and resuspended in RNase-free water.
824
825 **Quantitative reverse transcription real-time PCR**
826 Total RNA was treated with DNaseI (NEB) and processed with Superscript IV First
827 Strand Synthesis Systems (Life Technologies) using oligo (dT) primers following the
828 recommendations of the manufacturer. Real-time PCR was done with iTaq Universal
829 SYBR Green Supermix (BioRad) according to the recommendations of the
830 manufacturer. C_t normalization was done using *act-1*. All primer sequences are listed in
831 Key Resources Table.
832

QUANTIFICATION AND STATISTICAL ANALYSIS

Statistical significance was determined using Prism 8 (GraphPad Software) using the statistical tests indicated in the figure legends.

DATA AND SOFTWARE AVAILABILITY

Not applicable.

842 **Supplemental figure legends**

843 **Figure S1.** GLP-4 is required in multiple tissues to regulate adult reproductive
844 plasticity. Brood size comparison of PD_{Stv} relative to CON_{Stv} in wild-type N2, *glp-4(bn2)*,
845 and tissue-specific rescue strains of *glp-4*. Assays were done at 15ºC from at least
846 three biological independent trials. *** $p < 0.001$, **** $p < 0.0001$, and specified *p*-value
847 (Student's *t*-test) refer to the comparison of PD_{Stv} to CON_{Stv} of a given genotype. $^{\&\&\&}$ $p <$
848 0.001 and $^{\&\&\&\&}$ $p < 0.0001$ (one-way ANOVA with Fisher's LSD test) refer to the
849 PD_{Stv}/CON_{Stv} brood size change between a given mutant genotype to wild-type N2. $^{\#}$ p
850 < 0.05 and n.s. (one-way ANOVA with Fisher's LSD test) refer to the PD_{Stv}/CON_{Stv}
851 brood size change between *glp-4(bn2)* and the indicated *glp-4* tissue-specific MosSCI
852 rescues. Additional brood size data is provided in Supplemental Table S11.

853

854 **Figure S2.** Differentially expressed N2 PD_{Stv} genes are enriched for DAF-16 targets.
855 (*A*) Venn diagram depicting overlap of DAF-16 and PQM-1 targets (Tepper et al. 2013)
856 with differentially expressed N2 PD_{Stv} genes compared to CON_{Stv} adults (Ow et al.
857 2018). See Supplemental Table S3. (*B*) Venn diagram comparing DAF-16 and TCER-1
858 targets with functions in lipid metabolism from germ line-less *glp-1(e2141ts)* animals
859 (Amrit et al. 2016) with differentially expressed N2 PD_{Stv} genes compared to CON_{Stv}
860 adults (Ow et al. 2018). See Supplemental Table S5.

861

862 **Figure S3.** Brood size comparison of PD_{Stv} grown in the presence of 40 nM of Δ^7-
863 dafachronic acid (Δ^7-DA) relative to the brood size of PD_{Stv} grown in the absence of Δ^7-
864 DA of wild-type N2, *kri-1(ok1251)*, and *tcer-1(tm1425)* strains. *p*-values (Student's *t*-test)

865 indicate the comparison between PD_{Stv} with Δ^7-DA to PD_{Stv} without Δ^7-DA of a given
866 genotype. Assays were done at 20°C from three independent biological replicates.
867 Additional brood size data is provided in Supplemental Table S12.
868
869 **Figure S4.** Reverse transcription quantitative PCR (qRT-PCR) measurements of the
870 of the levels of *vit-1*, *vit-2*, *vit-3/4/5*, and *vit-6* mRNA in one-day-old-adults following
871 RNAi-by-feeding of *k09f5.2* (*vit-1*). *act-1* was used as the normalization control. **** $p <$
872 0.0001 and n.s. (no significance) (Student's *t*-test) refer to the comparison of PD_{Stv} to
873 CON_{Stv} for a given RNAi knockdown. Primer sequences are provided in Supplemental
874 Table S16.
875
876 **Figure S5.** DAF-12 acts downstream of TCER-1 and KRI-1. Brood size comparison of
877 PD_{Stv} relative to CON_{Stv} for wild-type N2, *kri-1(ok1251); daf-12(rh284)*, *tcer-1(tm1425);*
878 *dat-12(rh284)*, *kri-1(ok1251); daf-12(rh285)*, and *tcer-1(tm1425); dat-12(rh285)*. * $p <$
879 0.05; *** $p < 0.001$, **** $p < 0.0001$ (Student's *t*-test) indicates the brood size
880 comparison between PD_{Stv} relative to CON_{Stv} of a given genotype. &&&& $p < 0.0001$ (one-
881 way ANOVA with Fisher's LSD test) indicates the comparison of PD_{Stv}/CON_{Stv} brood
882 size change between a given genotype to wild-type N2. Assays were performed at 20°C
883 from at least three independent biological replicates. Additional brood size data is
884 provided in Supplemental Table S10.
885
886 **Figure S6.** DAF-36 and TCER-1 are required for the delay in the onset of proliferation
887 in animals that have experienced starvation-induced dauer formation. (*A*) The number

888 of meiotic (transition zone) cell rows in CON_{Stv} and PD_{Stv} wild-type N2, *daf-36(k114),*
889 *nhr-49(nr2041)*, and *tcer-1(tm1452)* at L3 stage was determined by counting the germ
890 cells rows that express the crescent shaped morphology in DAPI stained worms. (*B*)
891 The number of mitotic cell rows in CON_{Stv} and PD_{Stv} wild-type N2, *daf-36(k114), nhr-*
892 *49(nr2041)*, and *tcer-1(tm1452)* at L3 stage was determined by subtracting the meiotic
893 cell rows from the total cell rows for each animal. Student's *t*-test comparison between
894 CON_{Stv} and PD_{Stv} of the same genotype: * p <0.05, ** p < 0.01, **** p < 0.0001. Sample
895 size is > 51 from at least three independent trials.
896
897 **Figure S7.** Wild *C. elegans* isolates exhibit adult reproductive plasticity. Brood size
898 comparison of PD_{Stv} relative to CON_{Stv} for *C. elegans* N2 Bristol, *C. briggsae* AF16, *C.*
899 *elegans* AB1, CB4856, ED3040, JU440, KR314, and TR403. * p < 0.05; ** p < 0.01, ***
900 p < 0.001, **** p < 0.0001 (Student's *t*-test) indicate the brood size comparison between
901 PD_{Stv} relative to CON_{Stv} of a given genotype. Assays were performed at 20°C from at
902 least three biologically independent replicates. Additional brood size data is provided in
903 Supplemental Table S13.
904
905
906 **References**

907 Almeida MV, Andrade-Navarro MA, Ketting RF. 2019. Function and evolution of
908 nematode RNAi pathways. RNA 5: 1-25.
909 Amrit FR, Steenkiste EM, Ratnappan R, Chen SW, McClendon TB, Kostka D, Yanowitz
910 J, Olsen CP, Ghazi A. 2016. DAF-16 and TCER-1 facilitate adaptation to

911 germline loss by restoring lipid homeostasis and repressing reproductive
912 physiology in C. elegans. PLoS Genet 12: e1005788.
913 Antebi A, Yeh WH, Tait D, Hedgecock EM, Riddle DL. 2000. daf-12 encodes a nuclear
914 receptor that regulates the dauer diapause and developmental age in C. elegans.
915 Genes Dev 14: 1512-1527.
916 Antebi A. 2014. Nuclear receptor signal transduction in C. elegans. in WormBook (ed.
917 The C. elegans research community), doi/10.1895/wormbook.1.64.2.
918 Arantes-Oliveira N, Apfeld J, Dillin A, Kenyon C. 2002. Regulation of life-span by germ-
919 line stem cells in Caenorhabditis elegans. Science 295: 502-505.
920 Berman JR, Kenyon C. 2006. Germ-cell loss extends C. elegans life span through
921 regulation of DAF-16 by kri-1 and lipophilic-hormone signaling. Cell 124: 1055-
922 1068.
923 Binder EB, Bradley RG, Liu W, Epstein MP, Deveau TC, Mercer KB, Tang Y, Gillespie
924 CF, Heim CM, Nemeroff CB, Schwartz AC. Association of FKBP5 polymorphisms
925 and childhood abuse with risk of posttraumatic stress disorder symptoms in
926 adults. Jama. 2008 Mar 19;299(11):1291-305.
927 Brenner S. 1974. The genetics of Caenorhabditis elegans. Genetics 77: 71-94.
928 Brock TJ, Browse J, Watts JL. 2006. Genetic regulation of unsaturated fatty acid
929 composition in C. elegans. PLoS Genet 2: e108.
930 Buckley BA, Burkhart KB, Gu SG, Spracklin G, Kershner A, Fritz H, Kimble J, Fire A,
931 Kennedy S. 2012. A nuclear Argonaute promotes multigenerational epigenetic
932 inheritance and germline immortality. Nature 489: 447-451.

933 Byerly L, Cassada RC, Russell RL. 1976. Life-cycle of nematode Caenorhabditis
934 elegans. I. Wild-type growth and reproduction. Dev Biol 51: 23-33.
935 Canario L, Lundeheim N, Bijma P. 2017. The early-life environment of a pig shapes the
936 phenotypes of its social partners in adulthood. Heredity 118: 534-541.
937 Cassada RC, Russell RL. 1975. The dauerlarva, a post-embryonic developmental
938 variant of the nematode Caenorhabditis elegans. Dev Biol 46: 326-342.
939 Dantzer B, Dubuc C, Goncalves IB, Cram DL, Bennett NC, Ganswindt A, Heistermann
940 M, Duncan C, Gaynor D, Clutton-Brock TH. 2019. The development of individual
941 differences in cooperative behaviour: maternal glucocorticoid hormones alter
942 helping behaviour of offspring in wild meerkats. Phil Trans R Soc B 374:
943 20180117.
944 Devkota R, Svensk E, Ruiz M, Ståhlman M, Borén J, Pilon M. 2017. The adiponectin
945 receptor AdipoR2 and its Caenorhabditis elegans homolog PAQR-2 prevent
946 membrane rigidification by exogenous saturated fatty acids. PLoS Genet 13:
947 e1007004.
948 Feng X, Guang S. 2013. Small RNAs, RNAi and the inheritance of gene silencing in
949 Caenorhabditis elegans. J Genet Genomics 40: 153-160.
950 Folick A, Oakley HD, Yu Y, Armstrong EH, Kumari M, Sanor L, Moore DD, Ortlund EA,
951 Zechner R, Wang MC. 2015. Lysosomal signaling molecules regulate longevity in
952 Caenorhabditis elegans. Science 347: 83-86.
953 Fowler K, Partridge L. 1989. A cost of mating in female fruitflies. Nature 338: 760-761.

954 Frokjaer-Jensen C, Davis MW, Hopkins CE, Newman BJ, Thummel JM, Olesen SP,
955 Grunnet M, Jorgensen EM. 2008. Single-copy insertion of transgenes in
956 Caenorhabditis elegans. Nat Genet 40: 1375-1383.
957 Gerisch B, Antebi A. 2004. Hormonal signals produced by DAF-9/cytochrome P450
958 regulate C. elegans dauer diapause in response to environmental cues.
959 Development 131: 1765-1776.
960 Ghazi A, Henis-Korenblit S, Kenyon C. 2009. A transcription elongation factor that links
961 signals from the reproductive system to lifespan extension in Caenorhabditis
962 elegans. PLoS Genet 5: e1000639.
963 Gil EB, Malone Link E, Liu LX, Johnson CD, Lees JA.1999. Regulation of the insulin-like
964 developmental pathway of Caenorhabditis elegans by a homolog of the PTEN
965 tumor suppressor gene. Proc Natl Acad Sci USA 96: 2925-2930.
966 Goh GYS, Winter JJ, Bhanshali F, Doering KRS, Lai R, Lee K, Veal EA, Taubert S.
967 2018. NHR-49/HNF4 integrates regulation of fatty acid metabolism with a
968 protective transcriptional response to oxidative stress and fasting. Aging Cell 17:
969 e12743.
970 Goudeau J, Bellemin S, Toselli-Mollereau E, Shamalnasab M, Chen Y, Aguilaniu H.
971 2011. Fatty acid desaturation links germ cell loss to longevity through NHR
972 80/HNF4 in C. elegans. PLoS Biol 9: e1000599.
973 Grant B, Hirsh D. 1999. Receptor-mediated endocytosis in the Caenorhabditis elegans
974 oocyte. Mol Biol Cell 10: 4311-4326.
975 Hales CN, Barker DJ. 1992. Type 2 (non-insulin-dependent) diabetes mellitus: the thrifty
976 phenotype hypothesis. Diabetologia 35: 595-601.

977 Hall SE, Beverly M, Russ C, Nusbaum C, Sengupta P. 2010. A cellular memory of
978 developmental history generates phenotypic diversity in C. elegans. Curr Biol 20:
979 149-155.
980 Hall SE, Chirn GW, Lau NC, Sengupta P. 2013. RNAi pathways contribute to
981 developmental history-dependent phenotypic plasticity in C. elegans. RNA 19:
982 306-319.
983 Han S, Schroeder EA, Silva-García CG, Hebestreit K, Mair WB, Brunet A. 2017. Mono-
984 saturated fatty acids link H3K4me3 modifiers to C. elegans lifespan. Nature 544:
985 185-190.
986 Hansen M, Flatt T, Aguilaniu H. 2013. Reproduction, fat metabolism, and life span: what
987 is the connection? Cell Metab 17: 10-19.
988 Hsin C, Kenyon C. 1999. Signals from the reproductive system regulate the lifespan of
989 C. elegans. Nature 399: 362-366.
990 Hu Q, D'Amora DR, MacNeil LT, Walhout AJM, Kubiseski TJ. 2018. The Caenorhabditis
991 elegans oxidative stress response requires the NHR-49 transcription factor. G3
992 (Bethesda) 8: 3857-3863.
993 Judd ET, Wessels FJ, Drewry MD, Grove M, Wright K, Hahn DA, Hatle JD. 2011.
994 Ovariectomy in grasshoppers increases somatic storage, but proportional
995 allocation of ingested nutrients to somatic tissues is unchanged. Aging cell.
996 10(6):972-9.
997 Kaletsky R, Yao V, Williams A, Runnels AM, Tadych A, Zhou S, Troyanskaya OG,
998 Murphy CT. 2018. Transcriptome analysis of adult Caenorhabditis elegans cells
999 reveals tissue-specific gene and isoform expression. PLoS Genet. 14: e1007559.

1000 Kamath RS, Martinez-Campos M, Zipperlen P, Fraser AG, Ahringer J. 2001.
1001 Effectiveness of specific RNA-mediated interference through ingested double-
1002 stranded RNA in Caenorhabditis elegans. Genome Biol 2: RESEARCH0002.
1003 Kenyon C. 2010. A pathway that links reproductive status to lifespan in Caenorhabditis
1004 elegans. Ann N Y Acad Sci 1204: 156-162.
1005 Kenyon CJ. 2010b. The genetics of ageing. Nature 464: 504-512.
1006 Kimble J, Sharrock WJ. 1983. Tissue-specific synthesis of yolk proteins in
1007 Caenorhabditis elegans. Dev Biol 96: 189-196.
1008 Kimble J, Ward S. 1988. Germ-line development and fertilization. in The nematode
1009 Caenorhabditis elegans (ed. WB Wood), pp. 191-213. Cold Spring Harbor
1010 Laboratory Press, New York, NY.
1011 Kimble J, Crittenden SL. 2005. Germline proliferation and its control. in WormBook (ed.
1012 The C. elegans research community) doi/10.1895/ wormbook.1.13.1.
1013 Kirkwood TB. 1977. Evolution of aging. Nature 270: 301-304.
1014 Kishimoto S, Uno M, Okabe E, Nono M, Nishida E. 2017. Environmental stresses
1015 induce transgenerationally inheritable survival advantages via germline-to-soma
1016 communication in Caenorhabditis elegans. Nat Commun 8: 14031-14043.
1017 Lapierre LR, Hansen M. 2012. Lessons from C. elegans: signaling pathways for
1018 longevity. Trends Endocrinol Metab 23: 637-644.
1019 Lee K, Goh GY, Wong MA, Klassen TL, Taubert S. 2016 Gain-of-function alleles in
1020 Caenorhabditis elegans nuclear hormone receptor nhr-49 are functionally
1021 distinct. PLoS One 11: e0162708.

1022 L'Hernault, SW. 2006. Spermatogenesis. in WormBook (ed. The C. elegans research
1023 community) doi/10.1895/ wormbook.1.85.1.
1024 Lin K, Hsin H, Libina N, Kenyon C. 2001. Regulation of the Caenorhabditis elegans
1025 longevity protein DAF-16 by insulin/IGF-1 and germline signaling. Nat Genet 28:
1026 139-145.
1027 Lindblom TH, Pierce GJ, Sluder AE. 2001. A C. elegans orphan nuclear receptor
1028 contributes to xenobiotic resistance. Curr Biol 11: 864-868.
1029 Lumey LH, Stein AD, Susser E. 2011. Prenatal famine and adult health. Annu Rev
1030 Public Health 32: 237-262.
1031 Magner DB, Wollam J, Shen Y, Hoppe C, Li D, Latza C, Rottiers V, Hutter H, Antebi A.
1032 2013. The NHR-8 nuclear receptor regulates cholesterol and bile acid
1033 homeostasis in C. elegans. Cell Metab 18: 212-224.
1034 Mahanti P, Bose N, Bethke A, Judkins JC, Wollam J, Dumas KJ, Zimmerman AM,
1035 Campbell SL, Hu PJ, Antebi A, Schroeder FC. 2014. Comparative metabolomics
1036 reveals endogenous ligands of DAF-12, a nuclear hormone receptor, regulating
1037 C. elegans development and lifespan. Cell Metab 19: 73-83.
1038 Mihaylova VT, Borland CZ, Manjarrez L, Stern MJ, Sun H. 1999. The PTEN tumor
1039 suppressor homolog in Caenorhabditis elegans regulates longevity and dauer
1040 formation in an insulin receptor-like signaling pathway. Proc Natl Acad Sci USA
1041 96: 7427-7432.
1042 Moreno-Arriola E, El Hafidi M, Ortega-Cuéllar D, Carvajal K. 2016. AMP-activated
1043 protein kinase regulates oxidative metabolism in Caenorhabditis elegans through
1044 the NHR-49 and MDT-15 transcriptional regulators. PLoS One 11: e0148089.

1045 Murphy CT, Hu PJ. 2013. Insulin/insulin-like growth factor signaling in C. elegans. In
1046 WormBook (ed. The C. elegans research community)
1047 doi/10.1895/wormbook.1.164.1.
1048 Neel JV. 1962. Diabetes mellitus: a "thrifty" genotype rendered detrimental by
1049 "progress"? Am J Hum Genet 14: 353-362.
1050 Ni JZ, Kalinava N, Chen E, Huang A, Trinh T, Gu SG. 2016. A transgenerational role of
1051 the germline nuclear RNAi pathway in repressing heat stress-induced
1052 transcriptional activation in C. elegans. Epigenetics Chromatin 9: 3-15.
1053 Nomura T, Horikawa M, Shimamura S, Hashimoto T, Sakamoto K. 2010. Fat
1054 accumulation in Caenorhabditis elegans is mediated by SREBP homolog SBP-1
1055 Genes Nutr 5: 17-27.
1056 Ogg S, Ruvkun G. 1998. The C. elegans PTEN homolog, DAF-18, acts in the insulin
1057 receptor-like metabolic signaling pathway. Mol Cell 2: 887-893.
1058 O'Rourke EJ, Soukas AA, Carr CE, Ruvkun G. 2009. C. elegans major fats are stored in
1059 vesicles distinct from lysosome-related organelles. Cell Metab 10: 430-435.
1060 Ortiz MA, Noble D, Sorokin EP, Kimble J. 2014. A new dataset of spermatogenic vs.
1061 oogenic transcriptomes in the nematode Caenorhabditis elegans. G3 (Bethesda)
1062 4: 1765-1772.
1063 Ow MC, Borziak K, Nichitean AM, Dorus S, Hall SE. 2018. Early experiences mediate
1064 distinct adult gene expression and reproductive programs in Caenorhabditis
1065 elegans. PLoS Genet 14: e1007219.

1066 Painter R, Osmond C, Gluckman P, Hanson M, Phillips D, Roseboom T. 2008.
1067 Transgenerational effects of prenatal exposure to the Dutch famine on neonatal
1068 adiposity and health in later life. BJOG 115: 1243-1249.
1069 Papsdorf K, Brunet A. 2019. Linking lipid metabolism to chromatin regulation in aging.
1070 Trends Cell Biol 29: 97-116.
1071 Partridge L, Gems D, Withers DJ. 2005. Sex and death: what is the connection? Cell
1072 120: 461-472.
1073 Patel DS, Fang LL, Svy DK, Ruvkun G, Li W. 2008. Genetic identification of HSD-1, a
1074 conserved steroidogenic enzyme that directs larval development in
1075 Caenorhabditis elegans. Development 135: 2239-2249.
1076 Pathare PP, Lin A, Bornfeldt KE, Taubert S, Van Gilst MR. 2012. Coordinate regulation
1077 of lipid metabolism by novel nuclear receptor partnerships. PLoS Genet 8:
1078 e1002645.
1079 Pellegroms B. Van Dongen S, Van Dyck H, Luc L. 2009. Larval food stress differentially
1080 affects flight morphology in male and female speckled woods (Pararge aegeria).
1081 Ecol Entomol 34: 387-393.
1082 Pushpa K, Kumar GA, Subramaniam K. 2013. PUF-8 and TCER-1 are essential for
1083 normal levels of multiple mRNAs in the C. elegans germline. Development 140:
1084 1312-1320.
1085 Ratnappan R, Amrit FR, Chen SW, Gill H, Holden K, Ward J, Yamamoto KR, Olsen CP,
1086 Ghazi A. 2014. Germline signals deploy NHR-49 to modulate fatty-acid β-
1087 oxidation and desaturation in somatic tissues of C. elegans. PLoS Genet 10:
1088 e1004829.

1089 Rechavi O, Houri-Ze'evi L, Anava S, Goh WSS, Kerk SY, Hannon GJ, Hobert O. 2014.
1090 Starvation-induced transgenerational inheritance of small RNAs in C. elegans.
1091 Cell 158: 277-287.
1092 Rechavi O, Lev I. 2017. Principles of transgenerational small RNA inheritance in
1093 Caenorhabditis elegans. Curr Biol 27: R720-R730.
1094 Rottiers V, Motola DL, Gerisch B, Cummins CL, Nishiwaki K, Mangelsdorf DJ, Antebi A.
1095 2006. Hormonal control of C. elegans dauer formation and life span by a Rieske-
1096 like oxygenase. Dev Cell 10: 473-482.
1097 Schulenburg H, Félix MA. 2017. The natural biotic environment of Caenorhabditis
1098 elegans. Genetics 206: 55-86.
1099 Seah NE, de Magalhaes Filho, CD, Petrashen AP, Henderson HR, Laguer J, Gonzalez
1100 J, Dillin A, Hansen M, Lapierre LR. 2016. Autophagy-mediated longevity is
1101 modulated by lipoprotein biogenesis. Autophagy 12: 261-272.
1102 Seydoux G, Savage C, Greenwald I. 1993. Isolation and characterization of mutations
1103 causing abnormal eversion of the vulva in Caenorhabditis elegans. Dev Biol. 157:
1104 423-436.
1105 Shakes DC, Wu JC, Sadler PL, Laprade K, Moore LL, Noritake A, Chu DS. 2009.
1106 Spermatogenesis-specific features of the meiotic program in Caenorhabditis
1107 elegans. PLoS Genet. 5: e1000611.
1108 Shen Y, Wollam J, Magner D, Karalay O, Antebi A. 2012. A steroid receptor-
1109 microRNAswitch regulates life span in response to signals from the gonad.
1110 Science 338: 1472-1476.

1111 Smith CJ, Ryckman KK. 2015. Epigenetic and developmental influences on the risk of
1112 obesity, diabetes, and metabolic syndrome. Diabetes Metab Syndr Obes 8: 295-
1113 302.
1114 Solari F, Bourbon-Piffaut A, Masse I, Payrastre B, Chan AM, Billaud M. 2005. The
1115 human tumour suppressor PTEN regulates longevity and dauer formation in
1116 Caenorhabditis elegans. Oncogene 24: 20-27.
1117 Spieth J, Nettleton M, Zuckeraprison E, Lea K, Blumenthal T. 1991. Vitellogenin motifs
1118 conserved in nematodes and vertebrates. J Mol Evol 32: 429-438.
1119 Steinbaugh MJ, Narasimhan SD, Robida-Stubbs S, Moronetti Mazzeo LE, Dreyfuss JM,
1120 Hourihan JM, Raghavan P, Operaña TN, Esmaillie R, Blackwell TK. 2015. Lipid
1121 mediated regulation of SKN-1/Nrf in response to germ cell absence. Elife 4:
1122 e07836.
1123 Stiernagle T. 2006. Maintenance of C. elegans. in WormBook (ed. The C. elegans
1124 research community) doi/10.1895/wormbook.1.101.1.
1125 Sulston JE, Horvitz HR. 1977. Post-embryonic cell lineages of the nematode,
1126 Caenorhabditis elegans. Dev Biol 56: 110-156.
1127 Svensk E, Ståhlman M, Andersson CH, Johansson M, Borén J, Pilon M. 2013. PAQR-2
1128 regulates fatty acid desaturation during cold adaptation in C. elegans. PLoS
1129 Genet 9: e1003801.
1130 Taubert S, Van Gilst MR, Hansen M, Yamamoto KR. 2006. A Mediator subunit, MDT-
1131 15, integrates regulation of fatty acid metabolism by NHR-49-dependent and -
1132 independent pathways in C. elegans. Genes Dev 20: 1137-1149.

1133 Tauffenberger A, Parker JA. 2014. Heritable transmission of stress resistance by high
1134 dietary glucose in Caenorhabditis elegans. PLoS Genet 10: e1004346.
1135 Telang A, Wells MA. 2004. The effect of larval and adult nutrition on successful
1136 autogenous egg production by a mosquito. J Insect Physiol 50: 677-685.
1137 Tepper RG, Ashraf J, Kaletsky R, Kleemann G, Murphy CT, Bussemaker HJ. 2013.
1138 PQM-1 complements DAF-16 as a key transcriptional regulator of DAF-2-
1139 mediated development and longevity. Cell 154: 676-690.
1140 Vaag AA, Grunnet LG, Arora GP, Brøns C. 2012. The thrifty phenotype hypothesis
1141 revisited. Diabetologia 55: 2085-2088.
1142 Van Abeelen AF, Elias SG, Bossuyt PM, Grobbee DE, van der Schouw YT, Roseboom
1143 TJ, Uiterwaal CS. 2012. Famine exposure in the young and the risk of type 2
1144 diabetes in adulthood. Diabetes 61: 2255-2260.
1145 Van Gilst MR, Hadjivassiliou H, Jolly A, Yamamoto KR. 2005a. Nuclear hormone
1146 receptor NHR-49 controls fat consumption and fatty acid composition in C.
1147 elegans. PLoS Biol 3: e53.
1148 Veenendaal M, Painter R, de Rooij S, Bossuyt P, van der Post J, Gluckman P, Hanson
1149 M, Roseboom T. 2013. Transgenerational effects of prenatal exposure to the
1150 1944-45 Dutch famine. BJOG 120: 548-554.
1151 Vitikainen EIK, Thompson FJ, Marshall HH, Cant MA. 2019. Live long and prosper:
1152 durable benefits of early-life care in banded mongooses. Phil Trans R Soc B 374:
1153 20180114.
1154 Wang MC, O'Rourke E, Ruvkun G. 2008. Fat metabolism links germline stem cells and
1155 longevity in C. elegans. Science 322: 957-960.

1156 Ward S, Carrel JS. 1979. Fertilization and sperm competition in the nematode
1157 Caenorhabditis elegans. Dev Biol 73: 304-321.
1158 Watts JL, Ristow M. 2017. Lipid and carbohydrate metabolism in Caenorhabditis
1159 elegans. Genetics 207: 413-446.
1160 Weaver IC, Cervoni N, Champagne FA, D'Alessio AC, Sharma S, Seckl JR, Dymov S,
1161 Szyf M, Meaney MJ. 2004. Epigenetic programming by maternal behavior. Nat
1162 Neurosci 7: 847-854.
1163 Westendorp RGJ, Kirkwood TBL. 1998. Human longevity at the cost of reproductive
1164 success. Nature 396: 743-746.
1165 Williams GC. 1966. Natural selection, the costs of reproduction, and a refinement of
1166 Lack's principle. Am Nat 100: 687-690.
1167 Wolff S, Ma H, Burch D, Maciel GA, Hunter T, Dillin A. 2006. SMK-1, an essential
1168 regulator of DAF-16-mediated longevity. Cell 124: 1039-1053.
1169 Yamawaki TM, Berman JR, Suchanek-Kavipurapu M, McCormick M, Gaglia MM, Lee
1170 SJ, Kenyon C. 2010. The somatic reproductive tissues of C. elegans promote
1171 longevity through steroid hormone signaling. PLoS Biol. 8: e1000468.
1172 Yang F, Vought BW, Satterlee JS, Walker AK, Jim Sun ZY, Watts JL, DeBeaumont R,
1173 Saito RM, Hyberts SG, Yang S, et al. 2006. An ARC/Mediator subunit required
1174 for SREBP control of cholesterol and lipid homeostasis. Nature 442: 700-704.
1175 Yen K, Le TT, Bansal A, Narasimhan SD, Cheng JX, Tissenbaum HA. 2010. A
1176 comparative study of fat storage quantitation in nematode Caenorhabditis
1177 elegans using label and label-free methods. PLoS One 5: e12810.

1178 Zhao LQ, Zhu DH. 2014. Effects of environmental factors and appendage injury on the
1179 wing variation in the cricket Velarifictorus ornatus. J Insect Sci 14: 117.

Ow et al. Figure 1

A

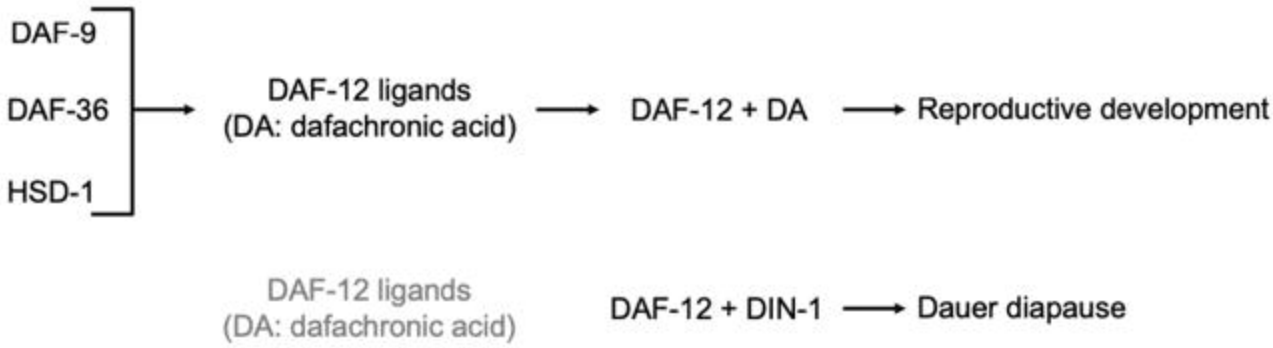

B

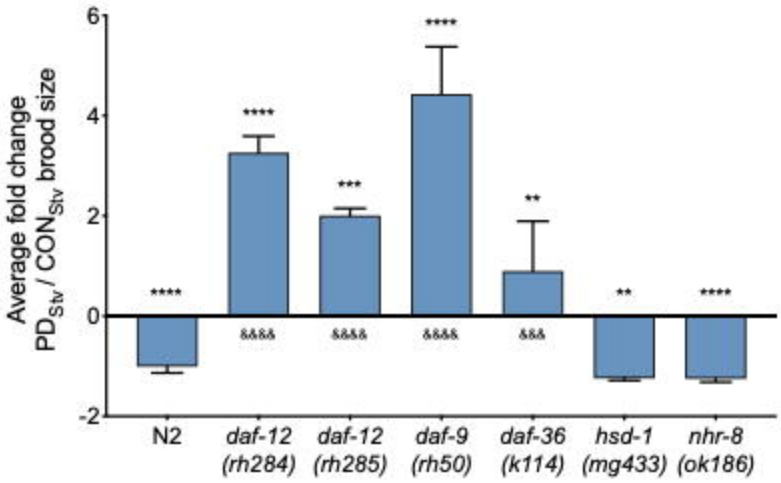

C

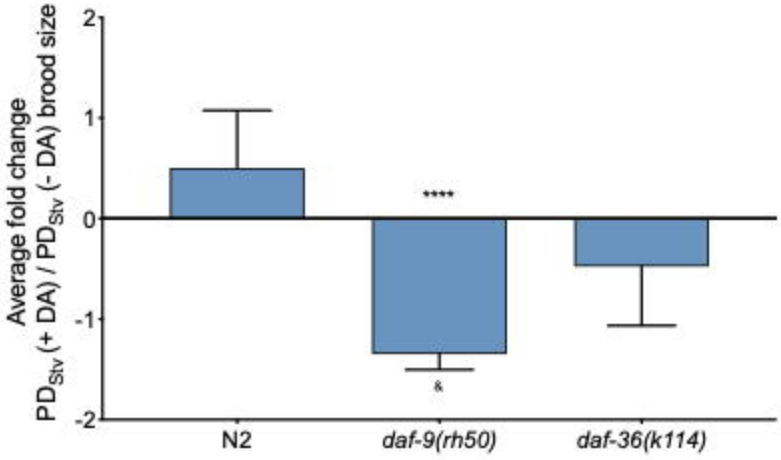

Ow et al. Figure 2

A

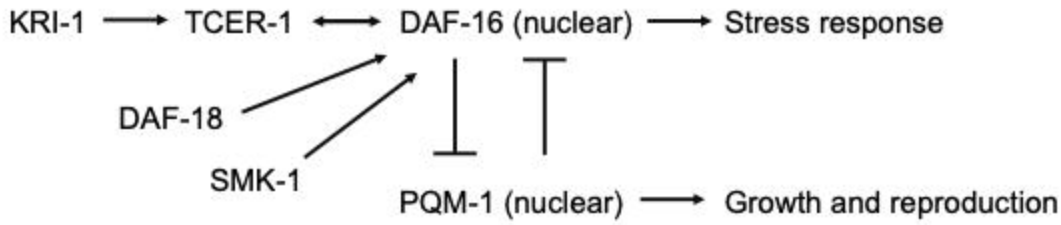

B

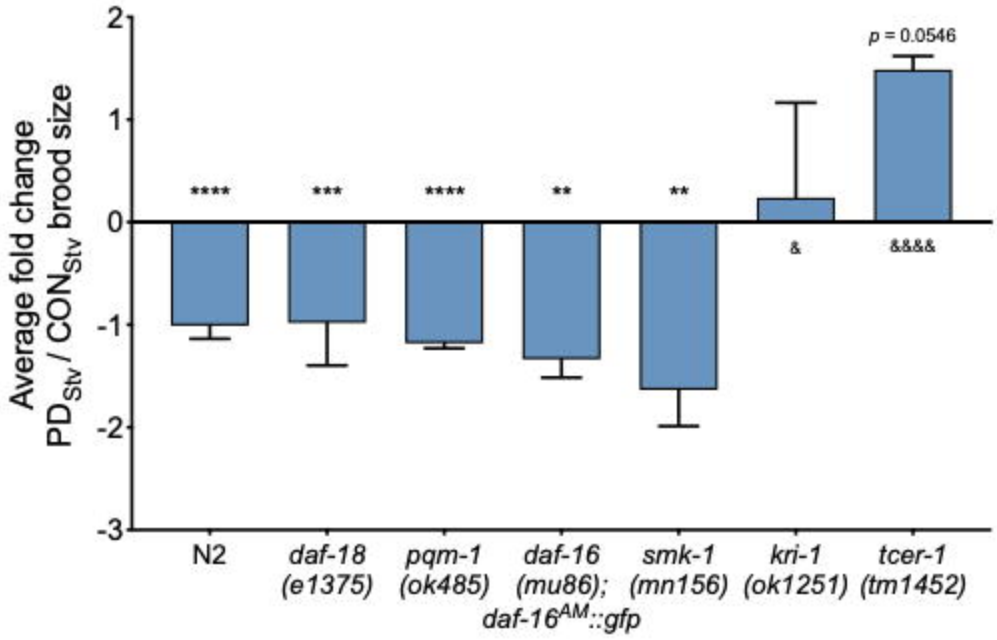

Ow et al. Figure 3

A

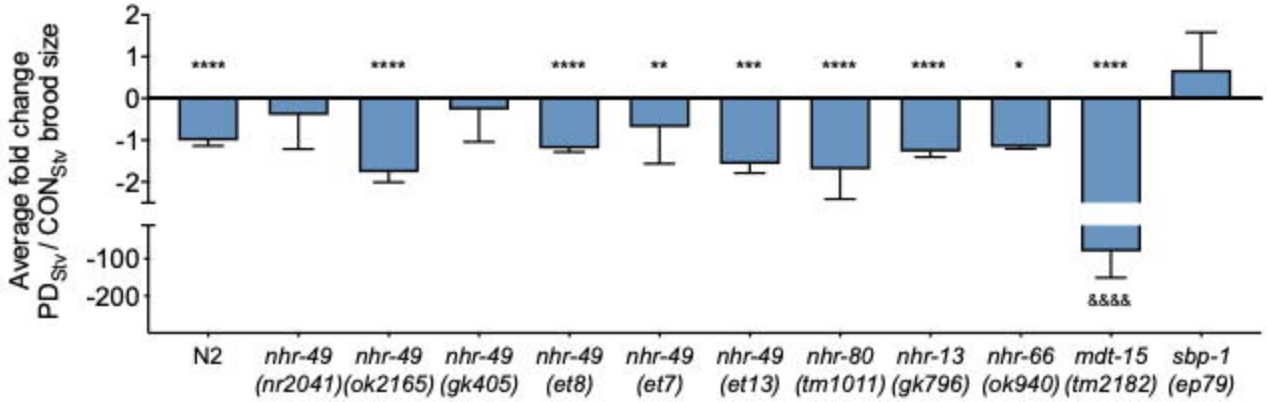

B

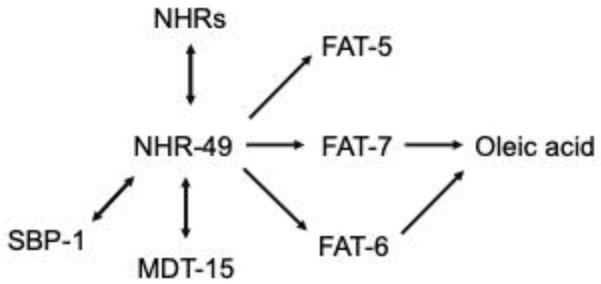

C

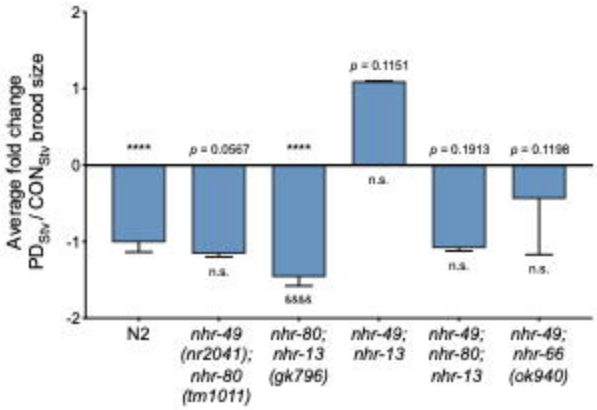

D

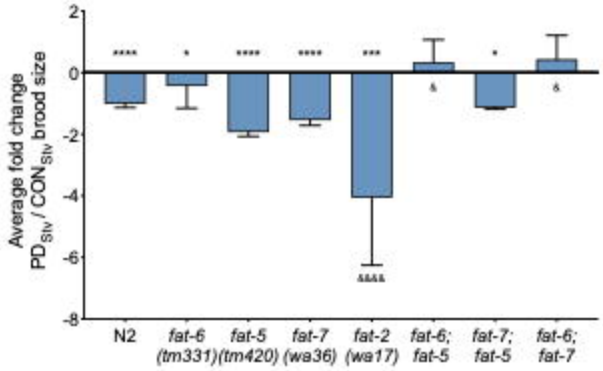

E

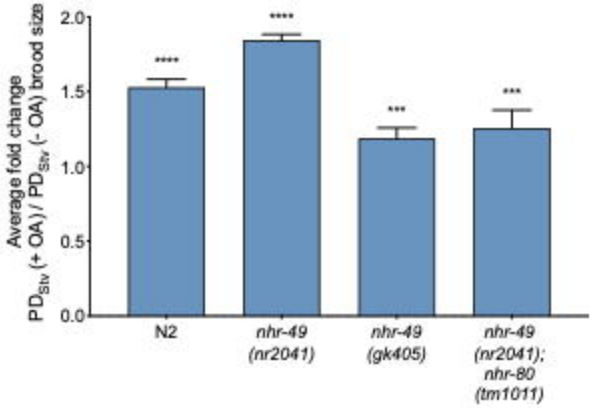

Ow et al. Figure 4

A

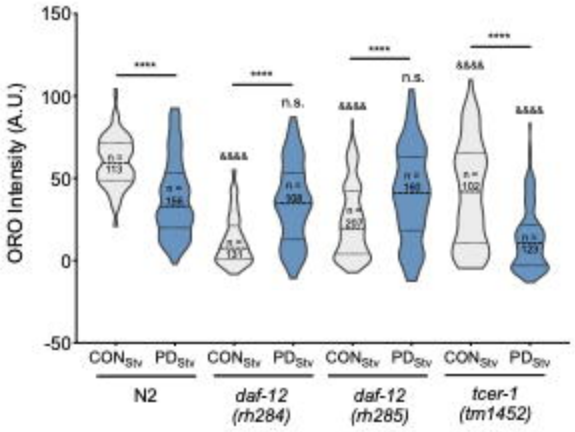

B

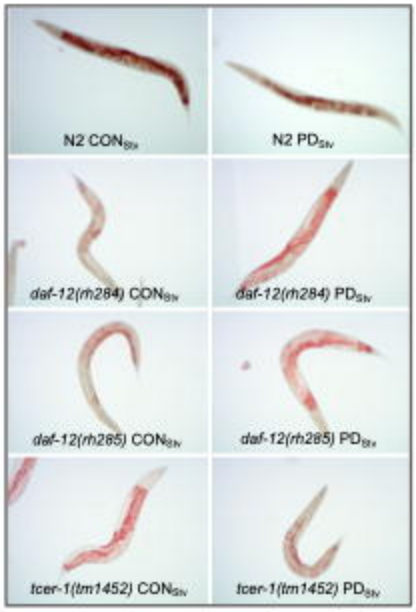

C

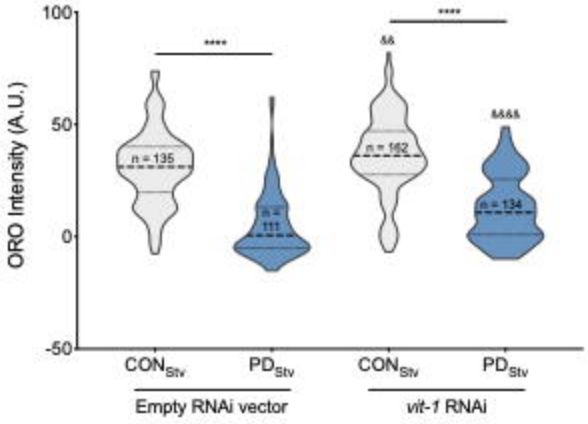

D

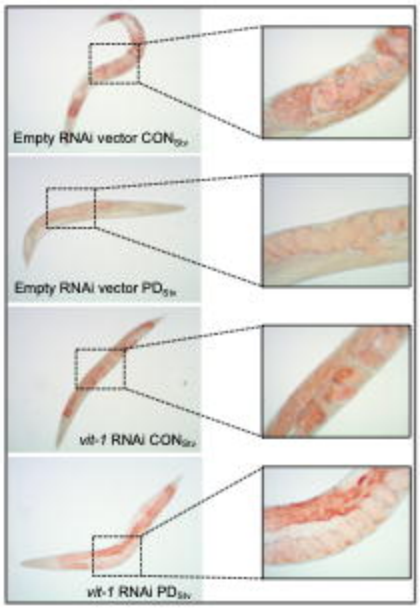

Ow et al. Figure 5

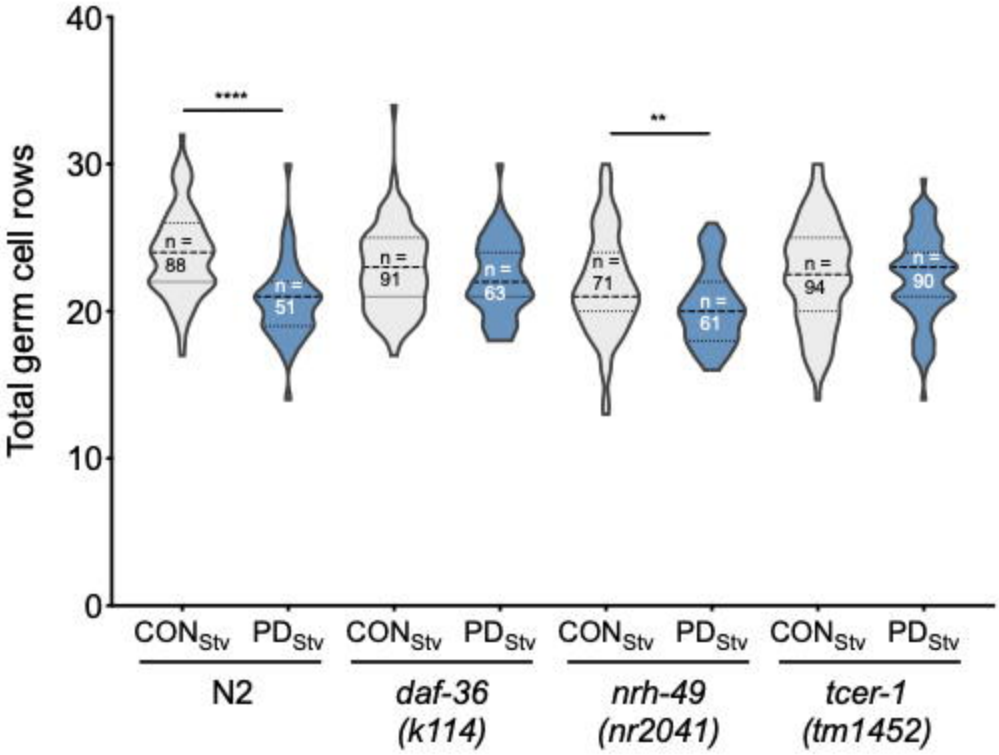

Ow et al. Figure 6

A

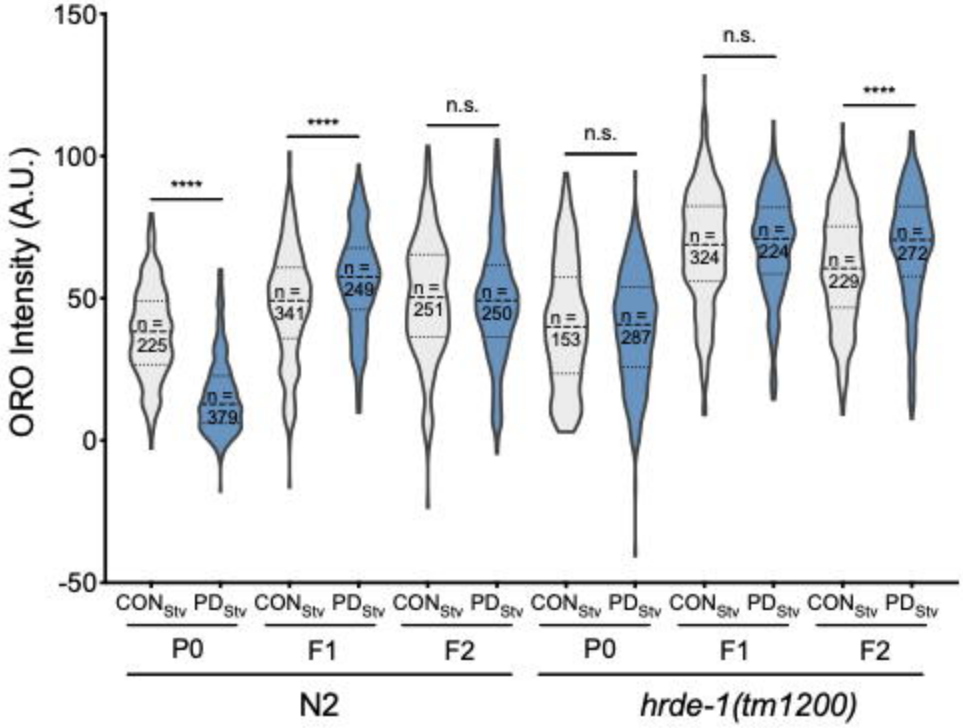

B

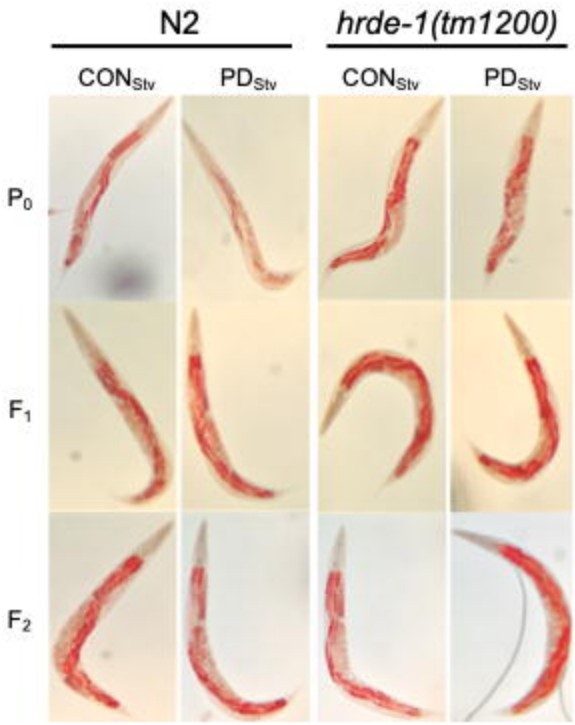

Ow et al. Figure 7

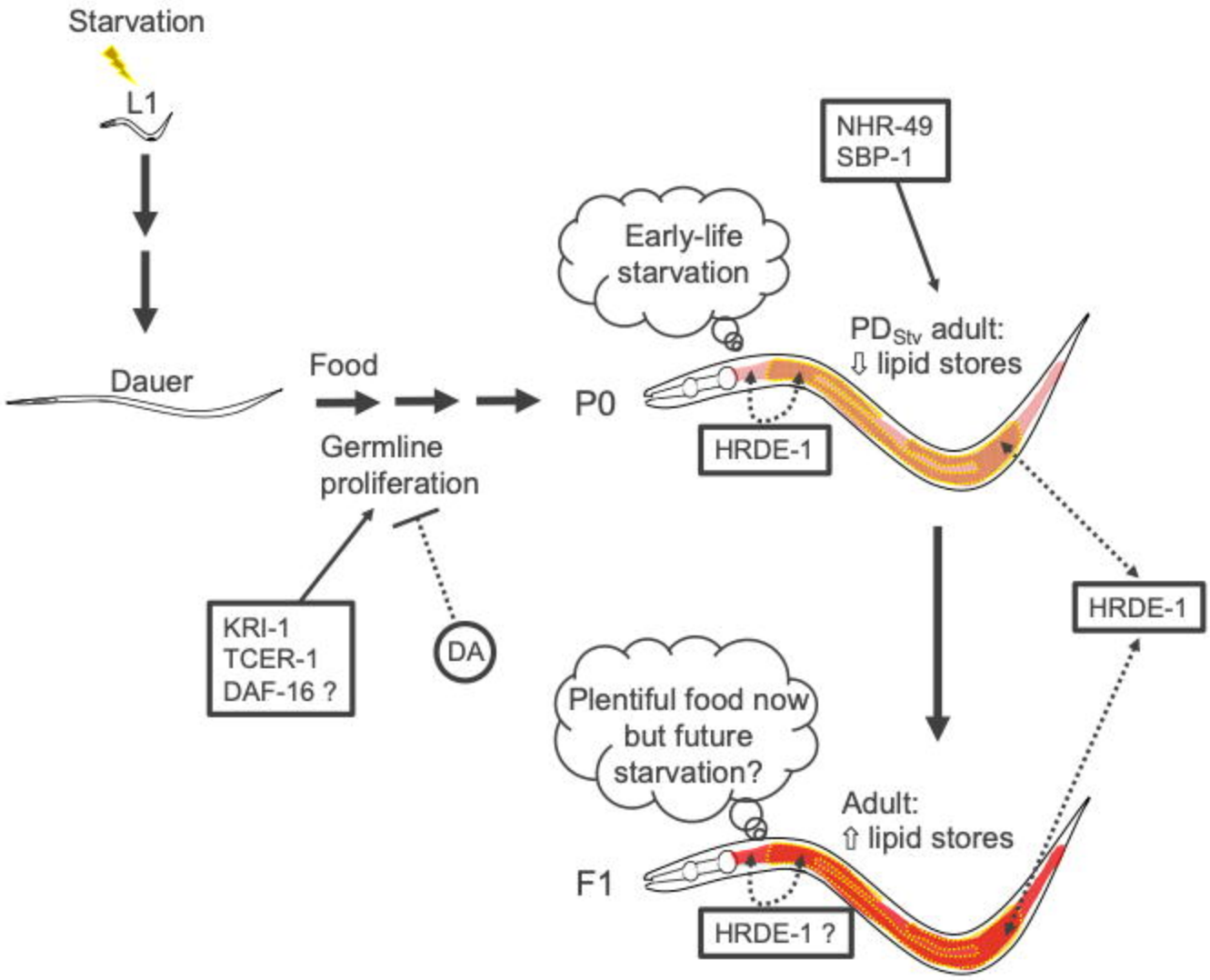

Ow et al. Supplemental Figure S1

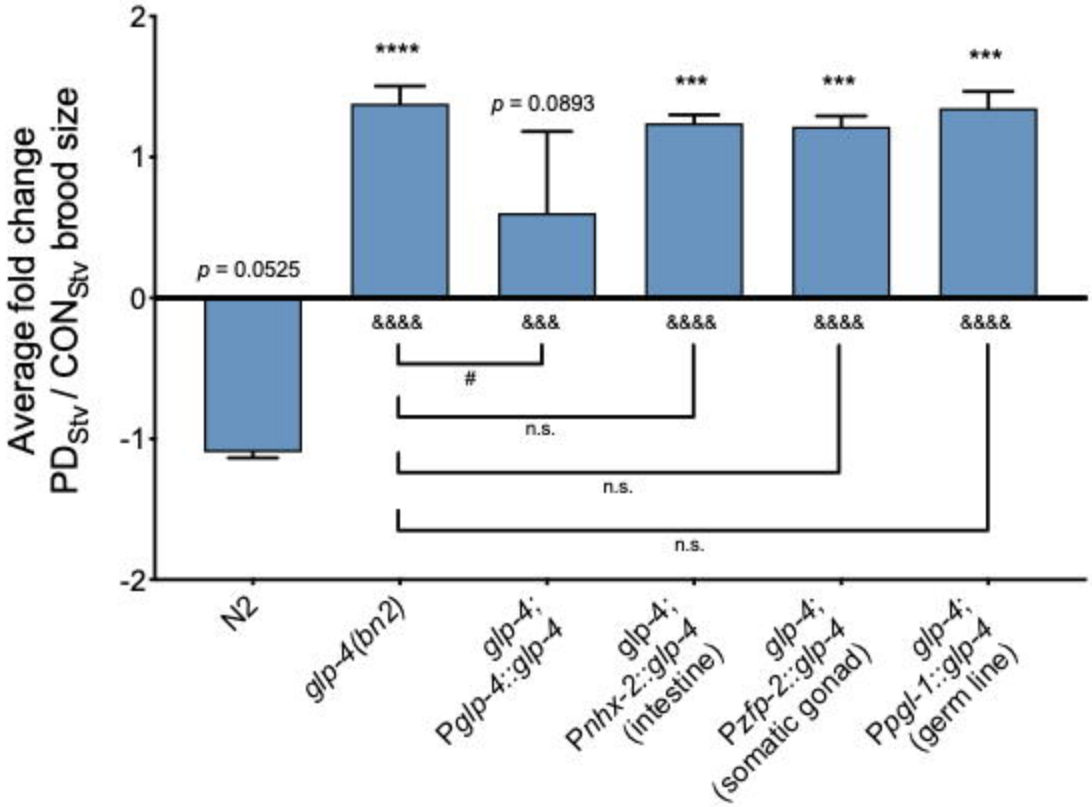

Ow et al. Supplemental Figure S2

A

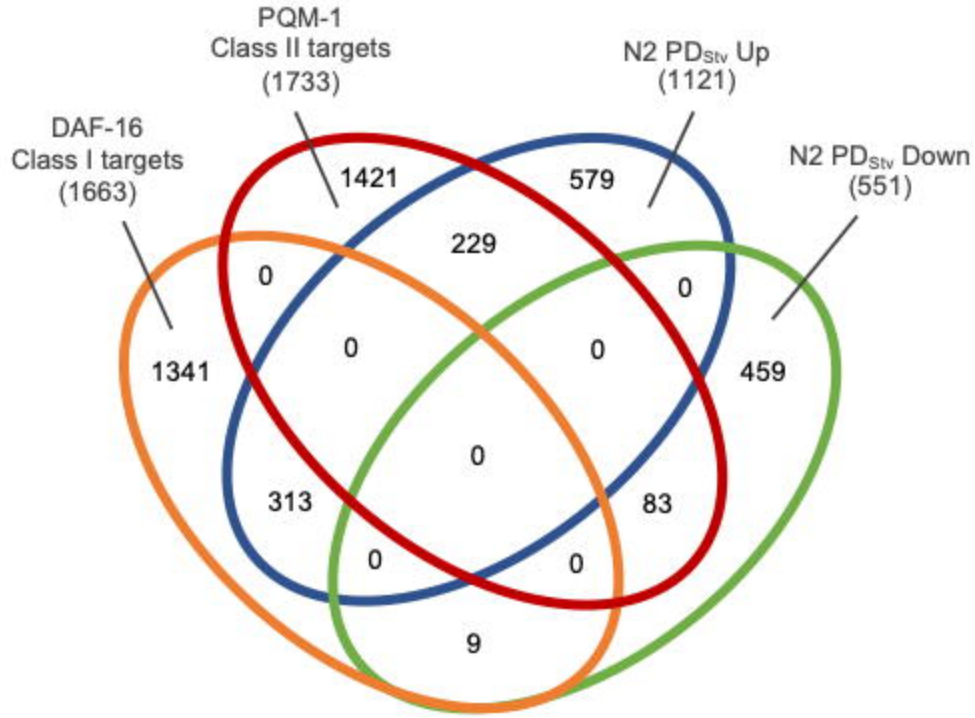

B

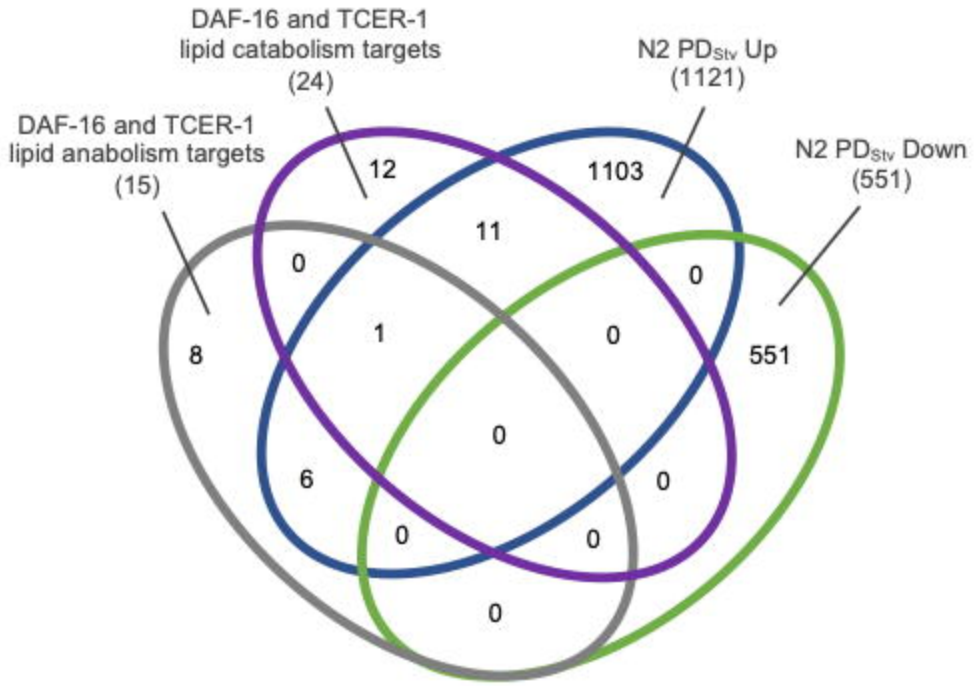

Ow et al. Supplemental Figure S3

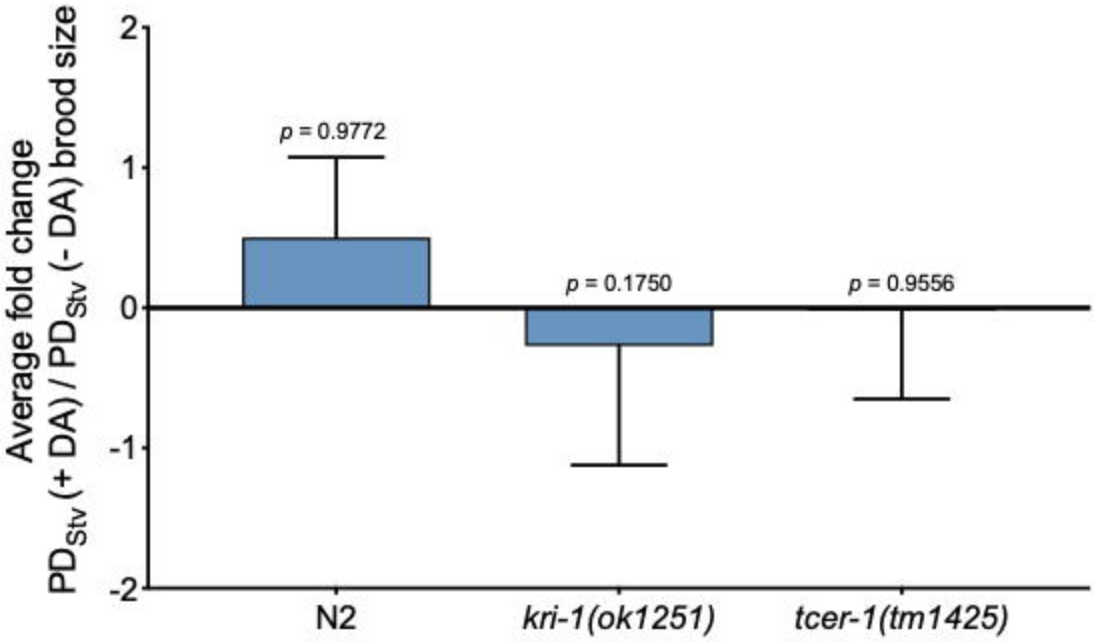

Ow et al. Supplemental Figure S4

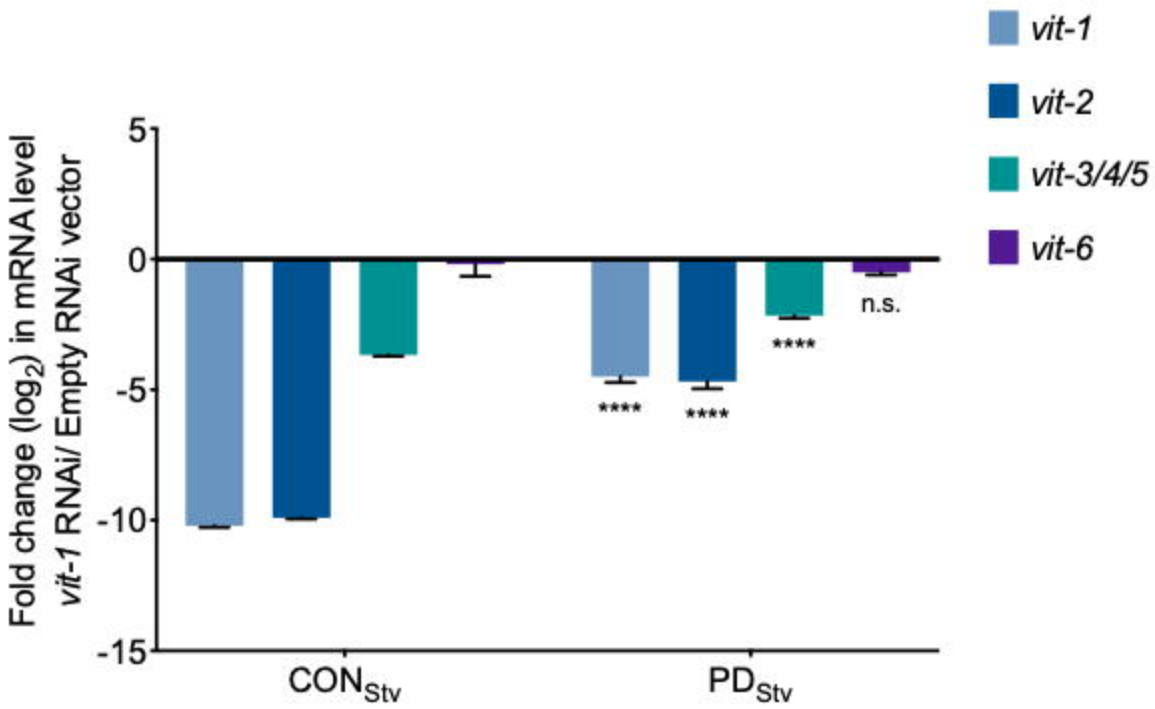

Ow et al. Supplemental Figure S5

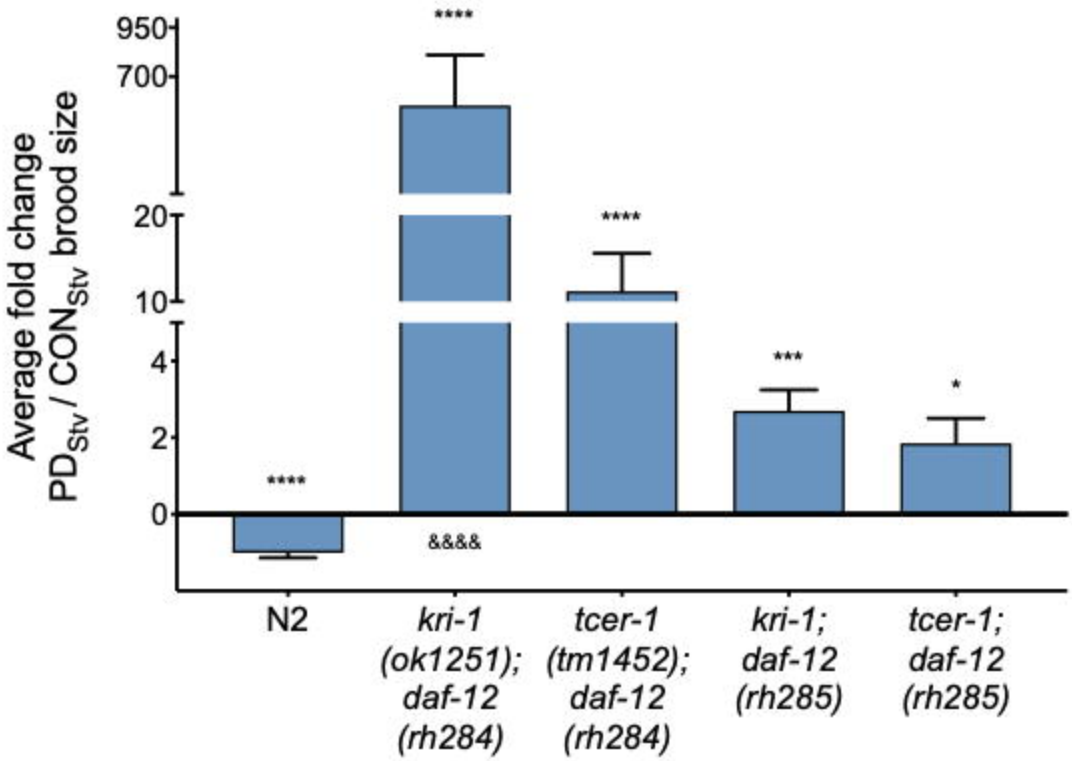

Ow et al. Supplemental Figure S6

A

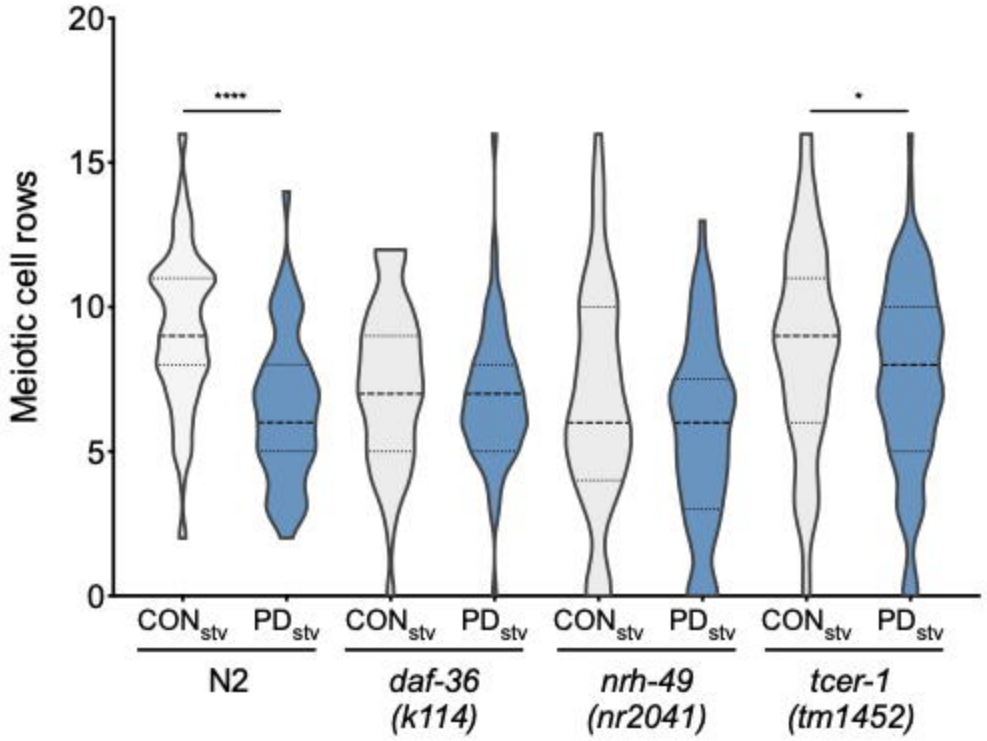

B

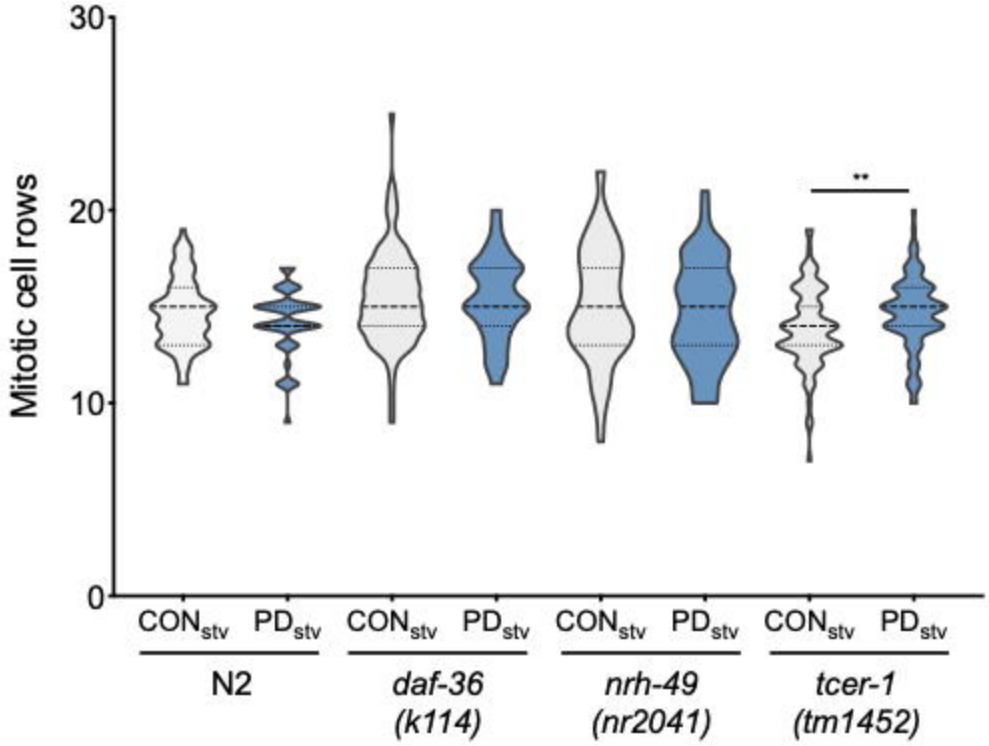
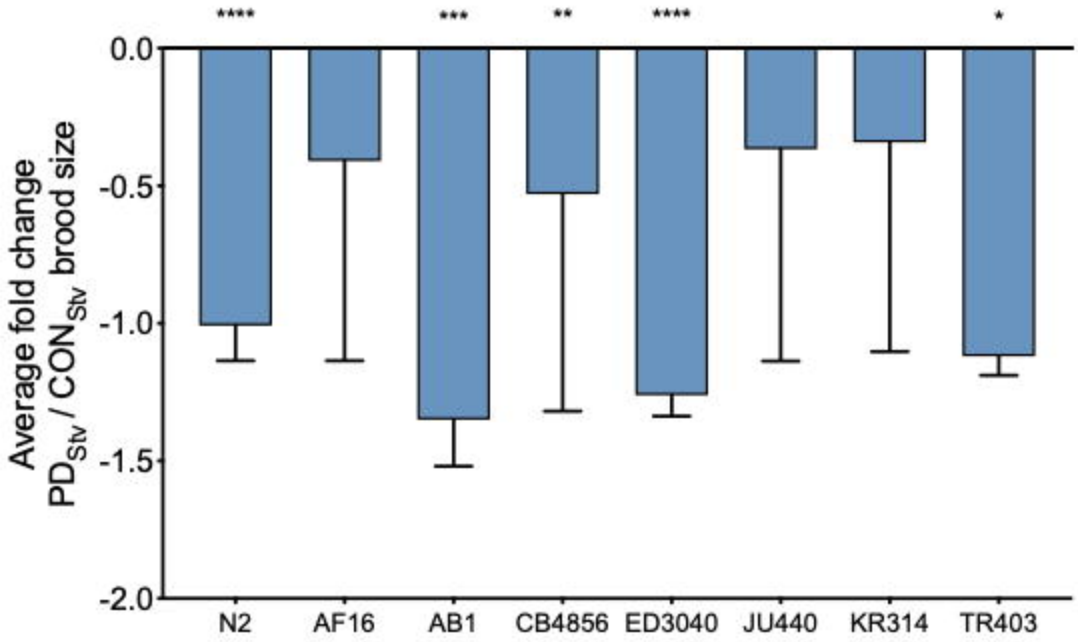
Ow et al. Supplemental Figure S7